ABSTRACT

In this thesis, a numerical method is presented for predicting transients in compressible fluid flow through a constant area circular channel. The fixed-grid method of characteristics is used to solve the differential equations governing the flow of the fluid. Several specific examples of practical interest are solved as an illustration of the method. It is further shown that this method, besides being much easier to program, also has an added advantage over the conventional approach. This advantage lies in the fact that the computed dependent variables are made available for all stations along the channel for fixed values of time. They are also available for fixed intervals of time at any station along the channel.

The method was programmed on IBM-360/65 digital computer at the University of Ottawa using Fortran IV language and a print out of the same appears in Appendix B. To demonstrate the usefulness of the technique, flow properties were computed at 51 equally spaced stations along a 1.86" diameter channel of 10 ft length for fixed time intervals of 0.0001 seconds. Realistic inlet and outlet conditions were prescribed. Results are presented in Chapter 4 of this thesis.

ACKNOWLEDGEMENT

This research project was carried out under the supervision of Dr. D. J. Gorman under whom I had the privilege of working as a graduate student towards my master's degree at the University of Ottawa. I am highly grateful to him for the encouragement, many constructive suggestions and countless hours he so willingly spent with me.

I gratefully acknowledge the financial support from the National Research Council of Canada and the Mechanical Engineering Department, University of Ottawa.

Finally, but by no means least, I wish to express a word of appreciation to my friend, Mr. R. K. Sharma, for his kind help and encouragement.

CONTENTS

LIST OF TABLES

INDEX OF FIGURES

NOMENCLATURE

		Units
a	Velocity of sound	ft/sec
A	Cross-sectional area	ft^2
C	Constant - see Eq. (2.10)	
C_p	Specific heat at constant pressure	Btu/lb^oR
C_v	Specific heat at constant volume	Btu/lb^oR
D	Diameter of the channel	ft
f	Friction factor	-
F	Frictional force per unit mass	lb_f/lb_m
F_1	Function - see Eq. (2.12)	lb_m/ft^2sec^2
g	Acceleration due to gravity	ft/sec^2
g_c	Newton constant relating force and mass	$\frac{ft}{sec^2}\left(\frac{lb_m}{lb_f}\right)$
G	Mass flow rate per unit area	lb/ft^2sec
h,k,w	Grid intercepts -see Eqs. (3.14), (3.16), (3.18), Fig. (4).	ft
J	Mechanical equivalent of heat	ft.lb/Btu
K	Wall friction factor	$(ft)^{-1}$
L	Channel length	ft
M	Number of stations	-
P	Pressure	lb/ft^2abs
q	Heat addition rate	Btu/lb.sec
Q_t	Function - see Eq. (2.6)	$(sec)^{-1}$
s	Specific entropy	Btu/lb^oR
R	Gas constant	$ft.lb/lb^oR$

		Units
S	Nondimensional entropy, $\frac{S}{C_v}$	-
t	Time	sec
z	Distance measured from channel inlet	ft
Δt	Time interval	sec
Δz	Distance interval	ft
γ	Ratio of specific heats(C_p/C_v)	-
ρ	Density	lb_m/ft^3
σ	Curve parameter	
τ_w	Wall shear stress	lb/ft^2

Subscripts

AT	Atmospheric
f	Final value
i,j	Grid coordinates
o	Refers to origin of grid ($z = 0$, $t = 0$)
L	Refers to $z = L$, $t = 0$

CHAPTER 1

INTRODUCTION

The analysis of one-dimensional flow transients is of great practical importance in nuclear power reactors. Such transients may occur, for example, with the rupture of a coolant channel or interruption of its coolant supply. In such cases it is necessary to predict accurately the changes with time of flow properties along the channel for reactor safety and design.

Efficient utilization of transient flow has been the subject of a great deal of research, as a result of which systems such as "Comprex" came into existence.

A solution to the differential equations governing the transient flow of a compressible fluid is usually obtained by the method of characteristics. In this method, most calculations are initiated along the first characteristic above which transient effects are felt. A series of starting points is selected and values for the variables are obtained for points on the time distance plane dictated by the intersection of characteristics drawn through the starting points. Beginning from pairs of newly established points the solution is advanced further out into the plane. Such solutions may be obtained by graphical or numerical means. Haller (3)* and Jenny (4) employed the graphical procedure while Kahane

---

*Numbers in parentheses refer to the references given at the end.

and Lees (5) and Rudinger (9) employed the numerical procedure for evaluating the flow variables along the characteristics. This conventional method has two serious shortcomings:

(1) The computational procedure becomes extremely involved due to the necessity of keeping track of all the computed points with their arbitrary and hence irregular positions on the time distance plane.

(2) Even with computation completed it is still not possible to plot the flow properties along the channel for fixed time intervals after the beginning of the transient. An involved interpolation of the values of the flow variables between the arbitrarily located points is required to achieve this end.

In the fixed-grid method of characteristics both of these shortcomings are overcome. Gorman and D'Arcy (2) employed this method wherein they utilized the continuity and momentum equations but neglected the energy equation. Their method, therefore, is approximate to that extent. The present investigation undertaken in this thesis also takes into account the energy equation. This method, therefore, can be regarded as an extension of their method.

The computational technique described here is shown to be a very accurate one for the study of single

phase diabatic transient flows of compressible fluids. It may be utilized with discretion for analyzing systems which do not completely meet these conditions.

To demonstrate the usefulness of the technique, flow properties were computed at 51 equally spaced stations along a 1.86" diameter channel of 10 ft length for fixed time intervals of 0.0001 seconds. Realistic inlet and outlet conditions were prescribed. Results are presented in Chapter 4 of this thesis.

CHAPTER 2

FORMULATION OF THE PROBLEM

A solution of a problem in compressible fluid flow requires the utilization of three equations, the continuity equation, the momentum equation, and the energy equation, together with an equation of state pertaining to the fluid. In the present analysis the transient flow of a compressible fluid through a constant area vertical channel with wall friction and heat addition has been considered. In order to simplify the analysis the following assumptions are made:

(i) the flow is one-dimensional and the properties of the fluid are set equal to their average values at each cross-section.

(ii) the fluid follows the perfect gas law and C_p and C_v are constant.

2.1 SELECTION OF FLOW VARIABLES

Because of one-dimensional approximation the kinetic properties of the fluid are represented by its average velocity at each cross-section or equivalently by its average mass flow rate (2). The flow is then completely defined by two state variables, e.g., density and specific entropy, and the mass flow rate, known at each cross-section at all times.

2.2 EQUATIONS OF MOTION

The equations of continuity and momentum have been derived in Appendix A. These take the following form:

CONTINUITY

$$\frac{\partial \rho}{\partial t} + \frac{\partial G}{\partial z} = 0 \tag{2.1}$$

MOMENTUM

$$\frac{\partial G}{\partial t} + \frac{\partial (G^2/\rho)}{\partial z} + g_c \frac{\partial P}{\partial z} + g\rho + \frac{K|G|G}{\rho} = 0 \tag{2.2}$$

ENERGY EQUATION

The entropy of a fluid particle changes according to heat added per unit mass and time, and also according to the work of friction per unit mass and unit time which is converted into heat (4).

$$ds = \frac{dQ}{T} = \frac{1}{T}\left[q + \frac{(G/\rho)F}{J}\right] dt$$

where

$F = \frac{K|G|G}{g_c \rho^2}$ represents the frictional force per unit mass, $\frac{lb_f}{lb_m}$

Dividing both sides by C_v and eliminating T by utilizing the relationship for velocity of sound

$$a^2 = g_c \gamma RT$$

we obtain, after substitution for F,

$$\frac{dS}{dt} = \frac{g_c \gamma R}{C_v a^2}\left[q + \frac{K|G|G^2}{\rho^3 g_c J}\right] \tag{2.3}$$

where $S = \frac{s}{C_v}$ represents nondimensional entropy.

For a perfect gas,

$$R = (C_p - C_v)J$$

or

$$\frac{R}{C_v} = (\gamma - 1)J \tag{2.4}$$

where R, the gas constant, is in mechanical units, ft.lb/lb$^{\circ}$R.

Eliminating R from Eq. (2.3) with the use of Eq. (2.4), we obtain

$$\frac{dS}{dt} = \frac{g_c \gamma(\gamma-1)J}{a^2}\left[q + \frac{K|G|G^2}{\rho^3 g_c J}\right]$$

or $$\frac{dS}{dt} = Q_t \tag{2.5}$$

where $$Q_t = \frac{g_c \gamma(\gamma-1)J}{a^2}\left[q + \frac{K|G|G^2}{\rho^3 g_c J}\right] \tag{2.6}$$

represents the rate of increase of entropy

and $\frac{d}{dt} \equiv \frac{\partial}{\partial t} + \frac{G}{\rho}\frac{\partial}{\partial z}$ represents the substantial derivative.

2.3 EQUATION OF STATE

The equation of state for a perfect gas is given by

$$P = \rho RT \tag{2.7}$$

where R is the gas constant.

The state variables used in the present analysis are ρ and S and therefore an equation of state of the form $P = P(\rho, S)$ is required.

According to the first law,

$$dq = C_v dT + P d(1/\rho) \tag{2.8}$$

where dq is the heat input for a small reversible process. Dividing Eq. (2.8) by T,

$$ds = \frac{dq}{T} = C_v \frac{dT}{T} + \frac{P}{T} d(1/\rho)$$

Utilizing Eq. (2.7), this Eq. becomes

$$ds = C_v \frac{d(P/\rho)}{(P/\rho)} + R \frac{d(1/\rho)}{(1/\rho)}$$

$$= C_v \frac{dP}{P} + C_p \frac{d(1/\rho)}{(1/\rho)}$$

Integrating and dividing throughout by C_v, we obtain

$$\frac{s-s_o}{C_v} = \ln\left(\frac{P}{P_o}\right) + \gamma \ln\left(\frac{1/\rho}{1/\rho_o}\right)$$

$$= \ln\left[\frac{P}{P_o}\left(\frac{\rho_o}{\rho}\right)^{\gamma}\right]$$

Taking exponential, we obtain, after simplication,

$$P = \left(\frac{P_o}{\rho_o^{\gamma} e^{S_o}}\right)\left(e^{S} \rho^{\gamma}\right)$$

or

$$P = C\, e^{S} \rho^{\gamma} \tag{2.9}$$

where

$$C = \frac{P_o}{\rho_o^{\gamma} e^{S_o}} = \text{constant}, \tag{2.10}$$

$$S = \frac{s}{C_v}$$

and subscript "o" represents the reference state from which entropy changes are measured.

2.4 DEVELOPMENT OF CHARACTERISTIC EQUATIONS

The variable P in Eq. (2.2) can be eliminated by the use of Eq. (2.9), thus reducing Eqs.(2.1), (2.2), (2.5) to a system of three quasi-linear partial differential equations of the first order and of the hyperbolic type in three dependent variables G, ρ, S. The method of characteristics may therefore be utilized to obtain a solution. To eliminate the derivative of P from Eq. (2.2) we proceed as follows:

Differentiating Eq. (2.9) partially with respect to z, we obtain

$$\frac{\partial P}{\partial z} = C\left[e^{S}.\gamma.\rho^{(\gamma-1)}\frac{\partial \rho}{\partial z} + \rho^{\gamma}e^{S}\frac{\partial S}{\partial z}\right]$$

$$= \frac{P\gamma}{\rho}\frac{\partial \rho}{z} + P\frac{\partial S}{\partial z}$$

Substitution of this in Eq. (2.2) yields

$$\frac{\partial G}{\partial t} + \frac{\partial (G^2/\rho)}{\partial z} + g_c\left(\frac{P\gamma}{\rho}\frac{\partial \rho}{\partial z} + P\frac{\partial S}{\partial z}\right) + g\rho + \frac{K|G|G}{\rho} = 0$$

Simplifying and utilizing the velocity of sound relationship

$$g_c\gamma\frac{P}{\rho} = a^2$$

this equation becomes

$$\frac{\partial G}{\partial t} + \frac{2G}{\rho}\frac{\partial G}{\partial z} + \left(a^2 - \frac{G^2}{\rho^2}\right)\frac{\partial \rho}{\partial z} + g_c Ce^S \rho^\gamma \frac{\partial S}{\partial z} + F_1 = 0 \qquad (2.11)$$

where

$$F_1 = g\rho + \frac{K|G|G}{\rho} \qquad (2.12)$$

Equations (2.1), (2.11) and (2.5) are rewritten for convenience as follows:

$$L_1 \equiv \frac{\partial G}{\partial z} + \frac{\partial \rho}{\partial t} = 0 \qquad (2.1)$$

$$L_2 \equiv \frac{\partial G}{\partial t} + \frac{2G}{\rho}\frac{\partial G}{\partial z} + \left(a^2 - \frac{G^2}{\rho^2}\right)\frac{\partial \rho}{\partial z} + g_c Ce^S \rho^\gamma \frac{\partial S}{\partial z} + F_1 = 0 \qquad (2.11)$$

$$L_3 \equiv \frac{\partial S}{\partial t} + \frac{G}{\rho}\frac{\partial S}{\partial z} - Q_t = 0 \qquad (2.5)$$

The integration of these equations in the present form is extremely difficult as the partial derivatives with respect to t and z are present. In order to make the integration possible we must change these equations into a simple form so that differentiations of G, ρ, and S occur only as total derivatives. This is achieved by following certain directions in the t-z plane depending on the point (t,z) as well as on the values of G, ρ, and S at this point. These are called "characteristic directions" (1).

In general, let us determine $\frac{df(x,y)}{ds'}$ when s' is as shown in Fig. 2(a).

$$\frac{df(x,y)}{ds'} = \frac{\partial f}{\partial x}\cdot\frac{dx}{ds'} + \frac{\partial f}{\partial y}\cdot\frac{dy}{ds'}$$

$$= \frac{\partial f}{\partial x}\cdot\frac{a}{\sqrt{a^2+b^2}} + \frac{\partial f}{\partial y}\cdot\frac{b}{\sqrt{a^2+b^2}}$$

or

$$\sqrt{a^2+b^2}\cdot\frac{df(x,y)}{ds'} = a\frac{\partial f}{\partial x} + b\frac{\partial f}{\partial y}$$

The term $\sqrt{a^2+b^2}$ being a scalar quantity will not affect the direction of differentiation. Therefore $a\frac{\partial f}{\partial x}+b\frac{\partial f}{\partial y}$ implies differentiation along s'.

Now if $\frac{dx}{d\sigma} / \frac{dy}{d\sigma} = \frac{a}{b}$ then $a\frac{\partial f}{\partial x} + b\frac{\partial f}{\partial y}$ is a derivative of $f(x,y)$ along the σ curve (see Fig. 2(b)). This curve is generated by a point moving with coordinates (x,y) such that $x = x(\sigma)$ and $y = y(\sigma)$. For example σ could be time, with x and y being functions of time.

Let us first consider the general case with two dependent variables where functions $u(x,y)$ and $v(x,y)$ are to be determined when $\frac{\partial u}{\partial x}$, $\frac{\partial u}{\partial y}$, $\frac{\partial v}{\partial x}$ and $\frac{\partial v}{\partial y}$ are given. Then the general form of the system of differential equations is (1)

$$L_1 = A_1\frac{\partial u}{\partial x} + B_1\frac{\partial u}{\partial y} + C_1\frac{\partial v}{\partial x} + D_1\frac{\partial v}{\partial y} + E_1 = 0 \qquad (2.13)$$

$$L_2 = A_2\frac{\partial u}{\partial x} + B_2\frac{\partial u}{\partial y} + C_2\frac{\partial v}{\partial x} + D_2\frac{\partial v}{\partial y} + E_2 = 0 \qquad (2.14)$$

where A_1, A_2, ... E_2 are known functions of x, y, u, v.

Consider the linear combination $L = \lambda_1 L_1 + \lambda_2 L_2$, where λ_1 and λ_2 are any functions of (x,y,u,v). By proper choice of λ_1 and λ_2 and hence the coefficients of $u_{,x}, u_{,y}$.

$v_{,x}$, $v_{,y}$ we can have direction of differentiation such that differentiation of u, in (x,y) plane and differentiation of v in (x,y) plane coincide. Let this desired direction be given by $\frac{dx}{d\sigma}$, $\frac{dy}{d\sigma}$. Then from previous argument we require

$$\frac{\lambda_1 A_1 + \lambda_2 A_2}{\lambda_1 B_1 + \lambda_2 B_2} = \frac{\lambda_1 C_1 + \lambda_2 C_2}{\lambda_1 D_1 + \lambda_2 D_2} = \frac{x_{,\sigma}}{y_{,\sigma}} \tag{2.15}$$

where $\frac{dx}{d\sigma}$ and $\frac{dy}{d\sigma}$ are written in the symbolic form as $x_{,\sigma}$ and $y_{,\sigma}$ respectively.

The preceding discussion of two dependent variables u and v and two independent variables x and y can be readily extended to include three dependent variables G, ρ and S and two independent variables z and t. Then the linear combination can be written as

$$L = \lambda_1 L_1 + \lambda_2 L_2 + \lambda_3 L_3 \tag{2.16}$$

Substitution of Eqs. (2.1), (2.11), (2.5) in (2.16) yields

$$L = \left[\lambda_2 \frac{\partial G}{\partial t} + \left(\lambda_1 + \frac{2G}{\rho}\lambda_2\right)\frac{\partial G}{\partial z}\right] + \left[\lambda_1 \frac{\partial \rho}{\partial t} + \lambda_2 \left(a^2 - \frac{G^2}{\rho^2}\right)\frac{\partial \rho}{\partial z}\right]$$

$$+ \left[\lambda_3 \frac{\partial S}{\partial t} + \left(\lambda_2 g_c C e^{S} \rho^{\gamma} + \frac{G}{\rho}\lambda_3\right)\frac{\partial S}{\partial z}\right] + \left[\lambda_2 F_1 - \lambda_3 Q_t\right] = 0 \tag{2.17}$$

The condition that in Eq. (2.17) G, ρ and S are differentiated along the same direction requires

$$\frac{\left(\lambda_1 + \frac{2G}{\rho}\lambda_2\right)}{\lambda_2} = \frac{\left(a^2 - \frac{G^2}{\rho^2}\right)\lambda 2}{\lambda_1} = \frac{\left(g_c C e^{S} \rho^{\gamma} \lambda_2 + \frac{G}{\rho}\lambda_3\right)}{\lambda_3} = \frac{z_{,\sigma}}{t_{,\sigma}} \tag{2.18}$$

Multiplying Eq. (2.17) by $t_{,\sigma}$ and utilizing Eq. (2.18), we obtain

$$t_{,\sigma}L = \lambda_2\left(\frac{\partial G}{\partial t}\, t_{,\sigma} + \frac{\partial G}{\partial z}\, z_{,\sigma}\right) + \lambda_1\left(\frac{\partial \rho}{\partial t}\, t_{,\sigma} + \frac{\partial \rho}{\partial z}\, z_{,\sigma}\right)$$

$$+ \lambda_3\left(\frac{\partial S}{\partial t}\, t_{,\sigma} + \frac{\partial S}{\partial z}\, z_{,\sigma}\right) + (\lambda_2 F_1 - \lambda_3 Q_t)\, t_{,\sigma} = 0$$

or

$$t_{,\sigma}L = \lambda_2 G_{,\sigma} + \lambda_1 \rho_{,\sigma} + \lambda_3 S_{,\sigma} + (\lambda_2 F_1 - \lambda_3 Q_t) t_{,\sigma} = 0 \qquad (2.19)$$

From Eqs. (2.18), (2.19) we obtain the following four homogeneous linear equations for λ_1, λ_2 and λ_3:

$$t_{,\sigma}\lambda_1 + \left(\frac{2G}{\rho}\, t_{,\sigma} - z_{,\sigma}\right)\lambda_2 = 0 \qquad (2.20)$$

$$- z_{,\sigma}\lambda_1 + \left(a^2 - \frac{G^2}{\rho^2}\right) t_{,\sigma}\lambda_2 = 0 \qquad (2.21)$$

$$\left(g_c C e^S \rho^\gamma\, t_{,\sigma}\right)\lambda_2 + \left(\frac{G}{\rho}\, t_{,\sigma} - z_{,\sigma}\right)\lambda_3 = 0 \qquad (2.22)$$

$$\rho_{,\sigma}\lambda_1 + (G_{,\sigma} + F_1 t_{,\sigma})\lambda_2 + (S_{,\sigma} - Q_t\, t_{,\sigma})\lambda_3 = 0 \qquad (2.23)$$

Existence of a non-trivial solution for λ_1, λ_2 and λ_3 requires the coefficient matrix of the equations to have rank not greater than two. From Eqs. (2.20), (2.21) and (2.22), we obtain

$$\begin{vmatrix} t_{,\sigma} & \left(\frac{2G}{\rho}\, t_{,\sigma} - z_{,\sigma}\right) & 0 \\ -z_{,\sigma} & \left(a^2 - \frac{G^2}{\rho^2}\right) t_{,\sigma} & 0 \\ 0 & g_c C e^S \rho^\gamma\, t_{,\sigma} & \left(\frac{G}{\rho}\, t_{,\sigma} - z_{,\sigma}\right) \end{vmatrix} = 0$$

Expanding the determinant and simplifying, we obtain

$$\left(z_{,\sigma} - \frac{G}{\rho}\, t_{,\sigma}\right)\left[\left(z_{,\sigma} - \frac{G}{\rho}\, t_{,\sigma}\right)^2 - a^2 (t_{,\sigma})^2\right] = 0$$

Writing $\frac{z_{,\sigma}}{t_{,\sigma}} = \phi$ this equation becomes

$$(t_{,\sigma})^3(\phi - \frac{G}{\rho})\left[(\phi - \frac{G}{\rho})^2 - a^2\right] = 0$$

which is a third-order equation for the slope ϕ and yields three real and distinct roots for ϕ. This indicates that our system of equations (2.1), (2.11), (2.5) is a totally hyperbolic type.

The three characteristic directions are:

$$\phi_+ = \frac{dz}{dt} = \frac{G}{\rho} + a \qquad (2.24)$$

which represents the C_+ characteristics

$$\phi_- = \frac{dz}{dt} = \frac{G}{\rho} - a \qquad (2.25)$$

which represents the C_- characteristics

and $$\phi_o = \frac{dz}{dt} = \frac{G}{\rho} \qquad (2.26)$$

which represents the particle path characteristics C_o.

To obtain relationships for the dependent variables along the characteristics we may set equal to zero the determinant of the coefficient matrix of any three, except the first three, equations (2.20), (2.21), (2.22), (2.23) (ref. 1).

From Eqs. (2.20), (2.22) and (2.23), we obtain

$$\begin{vmatrix} t_{,\sigma} & (\frac{2G}{\rho} t_{,\sigma} - z_{,\sigma}) & 0 \\ 0 & (g_c C e^{S} \rho^{\gamma} t_{,\sigma}) & (\frac{G}{\rho} t_{,\sigma} - z_{,\sigma}) \\ \rho_{,\sigma} & (G_{,\sigma} + F_1 t_{,\sigma}) & (S_{,\sigma} - Q_t t_{,\sigma}) \end{vmatrix} = 0$$

Expanding the determinant and simplifying, we obtain

$$(z_{,\sigma} - \frac{G}{\rho} t_{,\sigma})\left[(G_{,\sigma} + F_1 t_{,\sigma}) t_{,\sigma} - (\frac{2G}{\rho} t_{,\sigma} - z_{,\sigma}) \rho_{,\sigma}\right] +$$

$$g_c C e^{S} \rho^{\gamma} (t_{,\sigma})^2 (S_{,\sigma} - Q_t t_{,\sigma}) = 0$$

Writing $\frac{z_{,\sigma}}{t_{,\sigma}} = \phi$ this equation becomes

$$(t_{,\sigma})^2 \left\{(\phi - \frac{G}{\rho})\left[(G_{,\sigma} + F_1 t_{,\sigma}) - (\frac{2G}{\rho} - \phi)\rho_{,\sigma}\right] + g_c C e^{S} \rho^{\gamma} (S_{,\sigma} - Q_t t_{,\sigma})\right\} = 0 \qquad (2.27)$$

Therefore, along any C_+ characteristic defined by Eq. (2.24) the dependent variables are related by Eq. (2.27) with ϕ_+ used for ϕ. Introducing Eq. (2.24) into Eq. (2.27) and simplifying, we obtain

$$a\left[(G_{,\sigma} + F_1 t_{,\sigma}) - (\frac{G}{\rho} - a)\rho_{,\sigma}\right] + g_c C e^{S} \rho^{\gamma} (S_{,\sigma} - Q_t t_{,\sigma}) = 0$$

After utilizing the velocity of sound relationship $a^2 = \gamma g_c \frac{P}{\rho} = \gamma g_c C e^{S} \rho^{(\gamma-1)}$ this equation can be rewritten as

$$\frac{dG}{dt} - (\frac{G}{\rho} - a)\frac{d\rho}{dt} + \frac{\rho a}{\gamma}\frac{dS}{dt} + (F_1 - \frac{\rho a}{\gamma} Q_t) = 0 \qquad (2.28)$$

The relation of dependent variables along the C_- characteristic is obtained by introducing Eq. (2.25) into (2.27). We obtain, after simplification

$$(-a)\left[(G_{,\sigma} + F_1 t_{,\sigma}) - (\frac{G}{\rho} + a)\rho_{,\sigma}\right] + g_c C e^{S} \rho^{\gamma} (S_{,\sigma} - Q_t t_{,\sigma}) = 0$$

or

$$\frac{dG}{dt} - \left(\frac{G}{\rho} + a\right)\frac{d\rho}{dt} - \frac{\rho a}{\gamma}\frac{dS}{dt} + \left(F_1 + \frac{\rho a}{\gamma} Q_t\right) = 0 \qquad (2.29)$$

By introducing Eq. (2.26) into (2.27), we obtain the relationship of dependent variables along the particle path characteristics C_o. This is

$$g_c C e^{S} \rho^{\gamma} \left(S_{,\sigma} - Q_t\, t_{,\sigma}\right) = 0$$

or

$$\frac{dS}{dt} = Q_t \qquad (2.30)$$

which is in agreement with Eq. (2.5).

Thus, equations (2.1), (2.11) and (2.5) are equivalent to the system of ordinary equations:

C_+ :

$$\frac{dG}{dt} - \left(\frac{G}{\rho} - a\right)\frac{d\rho}{dt} + \left(\frac{\rho a}{\gamma}\right)\frac{dS}{dt} + \left(F_1 - \frac{\rho a}{\gamma} Q_t\right) = 0 \qquad (2.28)$$

$$\frac{dz}{dt} = \frac{G}{\rho} + a \qquad (2.24)$$

C_- :

$$\frac{dG}{dt} - \left(\frac{G}{\rho} + a\right)\frac{d\rho}{dt} - \left(\frac{\rho a}{\gamma}\right)\frac{dS}{dt} + \left(F_1 + \frac{\rho a}{\gamma} Q_t\right) = 0 \qquad (2.29)$$

$$\frac{dz}{dt} = \frac{G}{\rho} - a \qquad (2.25)$$

C_o : Particle path

$$\frac{dS}{dt} = Q_t \qquad (2.30)$$

$$\frac{dz}{dt} = \frac{G}{\rho} \qquad (2.26)$$

where $$F_1 = g\rho + \frac{K|G|G}{\rho} \tag{2.12}$$

$$Q_t = \frac{g_c\gamma(\gamma-1)J}{a^2}\left[q + \frac{K|G|G^2}{\rho^3 g_c J}\right] \tag{2.6}$$

$$a = \sqrt{\gamma g_c \frac{P}{\rho}} = \sqrt{\gamma g_c C e^{S\rho(\gamma-1)}} \tag{2.31}$$

and

$$C = \frac{P_o}{\rho_o^\gamma e^{S_o}} = \text{constant} \tag{2.10}$$

Equations (2.24), (2.25) and (2.26) define the characteristic directions C_+, C_- and C_o respectively. These directions define three families of characteristic curves or simply characteristics which cover the (t,z) plane. Equations (2.28), (2.29) and (2.30) are relations which must be satisfied by the solution G(t,z), ρ(t,z), S(t,z) along the respective characteristics.

2.5 INITIAL AND BOUNDARY CONDITIONS

In general, the initial conditions along a non-characteristic line AB($t = t_o$) (Fig. 3) determine the solution completely in the region bounded by the C_+ and C_- characteristics through A and B respectively and the line AB. In order to advance the solution beyond the region DAB it is necessary that solution is known along boundaries such as at A' and B'. In the case of subsonic flow considered here the C_+ characteristic has positive slope ($\frac{dz}{dt} > 0$) and C_- characteristic negative slope since $\frac{G}{\rho} + a$ is always positive and $\frac{G}{\rho} - a$ always negative. Thus C_- characteristic can only

reach the inlet end of the channel and C_+ characteristic can only reach the discharge end for increasing value of t.

In Fig. 3 let G represent a point for which all flow variables have already been determined. The C_- characteristic through G reaches the inlet end of the channel at a point A'. In order to compute three variables G, ρ, and S at A', three relations are required:

One relation is provided by equations (2.29), (2.25) of C_- characteristic and two boundary conditions including the entropy of the fluid must be prescribed at the inlet.

Let the flow conditions have already been determined for the points H and I near the discharge end. Two characteristics, C_+ and the particle path C_o, reach the discharge end at point B'. Thus two relations are provided by Eqs. (2.28), (2.24) and (2.30), (2.26) of these two charactersitics and only one boundary condition is required at the discharge end.

With known conditions at A' and B' the solution can be completely determined in the area A'B'D' and so on.

In this thesis the computational procedure was used to predict transients in air flow through a vertical circular channel. The flow field as well as the initial and temporal boundary conditions were specified as follows:

Pipe diameter, D = 1.86 in.

Pipe length, L = 10 ft.

Initial inlet air density, $\rho_o = 9.0$ lb/ft^3.

Initial mass flow rate, $G_o = 100$ lb/ft^2 sec.

Ratio of specific heats, $\gamma = 1.4$.

Gas constant, R = 53.35 ft lb/lb$^\circ$R.

Specific heat at constant volume C_v was calculated from the relation $C_v = R/(\gamma-1)J$, $C_v = 0.17143$ Btu/lb$^\circ$R.

Inlet entropy corresponding to P = 2000 psia and $\rho = 9.0$ lb/ft^3 was calculated with the help of Gas tables (6) as 0.289308 Btu/lb$^\circ$R. This value of entropy is reckoned from an arbitrary zero at T = 0°R and P = 1 atm.

The friction factor K was obtained from the Moody friction factor diagram (8) as 0.06 (ft)$^{-1}$ corresponding to flow through a pipe of 1.86 in. diameter and relative roughness = 5×10^{-4}.

Initially the flow was steady.

The boundary conditions as well as the heat addition rates were specified for different run numbers as tabulated below:

TABLE 1

The boundary conditions and the heat addition rates for various runs

Run No.	Heat Addition Rate (q) Btu/lb.sec	BOUNDARY CONDITIONS	
		Inlet End ($z = 0$)	Discharge End ($z = L$)
1	0	(i) $G(t,0)=G_o(1-\frac{t}{T})$ for $0 \leq t \leq T$ (2.32) which represents the inlet flow blockage. Flow reduction period, $T=0.2$ sec., i.e., $G(t,0)$ reduced from G_o to 0 in 0.2 sec. (ii) $S(t,0)=S_o=$const (2.33)	$\rho(t,L)=\rho_L=$const. (2.34)
2	30	Same as for run no.1	
3	0	(i) $\rho(t,0)=\rho_o=$const (2.35) (ii) $S(t,0)=S_o=$const (2.36)	$\rho(t,L)=\rho_L-(\rho_L-\rho_{AT})\frac{t}{T}$ for $\rho_L \geq \rho(t,L) \geq \rho_f$ where $\rho_f=7.635$ lb/ft^3 and, beyond this region $\rho(t,L)=\rho_f$ (2.37) which represents a discharge end rupture. The value of T was taken as 0.2 sec.
4	30	Same as for run no. 3	
5	0	Same as for run nos. 3 and 4	Same as for run nos. 3 and 4 except that $\rho_f = 7.5$ lb/ft^3

TABLE 1 (continued)

Run No.	Heat Addition Rate (q) Btu/lb.sec	BOUNDARY CONDITIONS	
		Inlet End ($z = 0$)	Discharge End ($z = L$)
6.	30	Same as for run nos. 3,4 and 5.	Same as for run no.5.
7	0	Same as for run nos. 3,4,5 and 6.	$P(t,L)=P_L-(P_L-P_{AT})\frac{t}{T}$ for $P_L \geq P(t,L) \geq P_f$ where $P_f = 1989.305$psia and, (2.38) beyond this region $P(t,L)=P_f$ which represents a discharge end rupture.
8	10	Same as for run nos. 3 through 7.	Same as for run no. 7.
9	30	Same as for run nos. 7 and 8.	
10	0	Same as for run nos. 3 through 9.	Same as for run nos. 7 through 9 except that $P_f = 1666.667$ psia.
11	30	Same as for run nos. 3 through 10.	Same as for run no. 10.

CHAPTER 3

COMPUTATIONAL PROCEDURE

3.1 FIXED GRID

The (t, z) plane was divided into a rectangular grid by the lines $t = t_i$, $z = z_j$ as shown in Fig. 4. Values of the three dependent variables G, ρ, and S were computed successively at the grid points, i.e., values of

$$G_{ij} \equiv G(t_i, z_j)$$
$$\rho_{ij} \equiv \rho(t_i, z_j)$$
$$S_{ij} \equiv S(t_i, z_j)$$

were computed.
Both t_i and z_j were equally spaced:

$$t_i = (i-1)\Delta t \qquad i = 1, 2, \ldots.$$
$$z_j = (j-1)\Delta z \qquad j = 1, 2, \ldots., M.$$

The pipe was divided into 50 segments of equal length giving 51 stations, i.e., M = 51, along the z axis.

Thus,

$$\text{station interval} = \Delta z = \frac{10}{50} = 0.2 \text{ ft.}$$

The time increment Δt is chosen from the consideration that the slope of the characteristics should be such that interceptions always occur within the station interval Δz. Referring to Eqs. (2.24), (2.25) and (2.26) of C_+, C_- and C_o characteristics, respectively, the condition for this is

$$\left|\frac{\Delta z}{\Delta t}\right| \geq \left|\frac{G}{\rho}\right| + a \tag{3.1}$$

$$\left|\frac{\Delta z}{\Delta t}\right| \geq \left|\frac{G}{\rho} - a\right| \tag{3.2}$$

$$\left|\frac{\Delta z}{\Delta t}\right| \geq \left|\frac{G}{\rho}\right| \tag{3.3}$$

G, ρ, and a, vary from station to station and as such the time increment. Δt is chosen such that

$$\Delta t \leq \frac{\Delta z}{\text{Max}\left(\left|\frac{G}{\rho}\right| + a\right)} \tag{3.4}$$

In the present work the value of Δt taken was 0.0001 sec.

3.2 INITIAL STEADY STATE CONDITIONS

Before computation for transient solution could be initiated it was necessary to solve for the initial steady state values of three dependent variables G, ρ, and S at 51 stations of the pipe.

For steady state conditions (t = 0) Eq. (2.1) takes the form:

$$\frac{dG}{dz} = 0$$

or, after integration,

$$G(0,z) = G_o = \text{constant} \tag{3.5}$$

where subscript "o" indicates inlet condition.

Writing Eqs. (2.11), (2.5) in finite difference form and for steady state, we obtain,

$$(a^2 - \frac{G^2}{\rho^2})\Delta\rho + g_c Ce^{S\rho^r}\Delta S + F_1\Delta z = 0 \qquad (3.6)$$

and $$\frac{G}{\rho}\Delta S - Q_t\Delta z = 0 \qquad (3.7)$$

Utilizing Eq. (3.5) in Eqs. (3.6) and (3.7), we obtain

$$(a^2 - \frac{G_o^2}{\rho^2})\Delta\rho + g_c Ce^{S\rho^r}\Delta S + F_1\Delta z = 0 \qquad (3.8)$$

where $$F_1 = g\rho + \frac{K|G_o|G_o}{\rho} \qquad (3.9)$$

and

$$\frac{G_o}{\rho}\Delta S - Q_t\Delta z = 0 \qquad (3.10)$$

where $$Q_t = \frac{g_c r(r-1)J}{a^2}\left[q + \frac{K|G_o|G_o^2}{\rho^3 g_c J}\right] \qquad (3.11)$$

Eliminating ΔS from Eq. (3.8) by use of Eq. (3.10),

$$(a^2 - \frac{G_o^2}{\rho^2})\Delta\rho + (\frac{g_c Ce^{S\rho^{(r+1)}}}{G_o}Q_t + F_1)\Delta z = 0 \qquad (3.12)$$

The values of $\rho_{1,2}$ and $S_{1,2}$ at station 2 are obtained as follows:

(i) Set $\rho_{1,2} = \rho_{1,1}$ ($\rho_{1,1}$ is specified)

and $S_{1,2} = S_{1,1}$ ($S_{1,1}$ is specified).

(ii) Compute F_1, a and Q_t.

(iii) Solve Eqs. (3.12) and (3.10) for $\Delta\rho$ and ΔS respectively.

(iv) Set $\rho_{1,2} = \rho_{1,1} + \Delta\rho$

and $S_{1,2} = S_{1,1} + \Delta S$

(v) Compute F_1, a and Q_t using mean values of ρ and S between the stations.

(vi) Solve Eqs. (3.12) and (3.10) for $\Delta\rho$ and ΔS, respectively, using mean values of ρ and S between the stations.

(vii) Set $\rho_{1,2} = \rho_{1,1} + \Delta\rho$,

$S_{1,2} = S_{1,1} + \Delta S$

and return to step (v).

(viii) Repeat computation until consecutive values of $\rho_{1,2}$ and $S_{1,2}$ agree within prescribed limits. The limits prescribed in the present work were $\pm 0.000001\ \rho$, ± 0.000001 S.

(ix) With $\rho_{1,2}$ and $S_{1,2}$ known solve for $\rho_{1,3}$ and $S_{1,3}$ etc.

3.3 TRANSIENT SOLUTION

The computation is initiated with known values of G, ρ, and S at the 51 stations, $j = 1,2,...51$, along the z axis ($i = 1$). Their values at the same 51 stations, after one time increment Δt, are obtained.

The procedure used for obtaining the values of G, ρ, and S at the 51 stations when $i > 1$ is broken into three parts.

3.3.1 SOLUTION AT INTERIOR STATIONS

Referring to Fig. 4, it is seen that the three characteristics C_+, C_- and C_o through the point (t_i, z_j) intercept the line $t = t_{i-1}$ at distances k, h, and w respectively from the station j. The value of Δt is small

enough so that interceptions always occur within the station interval Δz.

The procedure used when $1 < j < M$, $i > 1$ is as follows:

The derivatives $\frac{dG}{dt}$, $\frac{d\rho}{dt}$, $\frac{dS}{dt}$ and $\frac{dz}{dt}$ in Eqs. (2.28), (2.24), (2.29), (2.25), (2.30) and (2.26) are written in finite difference form as $\frac{\Delta G}{\Delta t}$, $\frac{\Delta \rho}{\Delta t}$, $\frac{\Delta S}{\Delta t}$ and $\frac{\Delta z}{\Delta t}$. Δt being the time increment is known. For C_+ characteristic, $\Delta z = k$, for C_- characteristic, $\Delta z = -h$, for C_o characteristic, $\Delta z = w$, where h, k and w are >0. Equations (2.28), (2.24), (2.29), (2.25), (2.30) and (2.26) written in finite difference form are six algebraic equations in the six unknowns G_{ij}, ρ_{ij}, S_{ij}, h, k, and w for any given value of i,j:

C_+ :

$$(G_{ij} - G_+) - \left(\overline{\frac{G}{\rho} - a}\right)_{ij,+} (\rho_{ij} - \rho_+) + \left(\overline{\frac{\rho a}{\gamma}}\right)_{ij,+} (S_{ij} - S_+) + \left[\overline{F_1 - \frac{\rho a Q_t}{\gamma}}\right]_{ij,+} \Delta t = 0 \qquad (3.13)$$

$$k - \left[\overline{\frac{G}{\rho} + a}\right]_{ij,+} \Delta t = 0 \qquad (3.14)$$

C_- :

$$(G_{ij}-G_-)-\left(\overline{\frac{G}{\rho}+a}\right)_{ij,-}(\rho_{ij}-\rho_-)-\left(\overline{\frac{\rho a}{\gamma}}\right)_{ij,-}(S_{ij}-S_-)$$

$$+\left[\overline{F_1+\frac{\rho a Q_t}{\gamma}}\right]_{ij,-}\Delta t = 0 \qquad (3.15)$$

$$-h-\left(\overline{\frac{G}{\rho}-a}\right)_{ij,-}\Delta t = 0 \qquad (3.16)$$

Particle Path C_o :

$$(S_{iJ}-S_p)-(\overline{Q_t})_{ij,p}\ \Delta t = 0 \qquad (3.17)$$

$$W-\left(\overline{\frac{G}{\rho}}\right)_{ij,p}\ \Delta t = 0 \qquad (3.18)$$

where, for any function $f(G,\rho,S)$,

$$\overline{f}_{ij,\pm} = \frac{1}{2}\left[f(G_{ij},\rho_{iJ},S_{ij}) + f(G_\pm,\rho_\pm,S_\pm)\right] \qquad (3.19)$$

$$\overline{f}_{ij,p} = \frac{1}{2}\left[f(G_{ij},\rho_{ij},S_{ij}) + f(G_p,\rho_p,S_p)\right] \qquad (3.20)$$

$$G_+ = G_{i-1,j} + \frac{k}{\Delta z}(G_{i-1,j-1} - G_{i-1,j}) \qquad (3.21)$$

$$G_- = G_{i-1,j} + \frac{h}{\Delta z}(G_{i-1,j+1} - G_{i-1,j}) \qquad (3.22)$$

$$G_p = G_{i-1,j} + \frac{w}{\Delta z}(G_{i-1,j-1} - G_{i-1,j}) \qquad (3.23)$$

and similarly for $\rho_\pm$, $S_\pm$, ρ_p and S_p. In the above equations

the subscripts +, - and p represent the conditions at points of intersections of C_+, C_- and C_o respectively on the line $t = t_{i-1}$ as shown in Fig. 4.

The method of solution for G_{ij}, ρ_{ij}, S_{ij} at the point (t_i, z_j) is:

(i) Set $G_{ij} = G_{i-1,j}$, $\rho_{ij} = \rho_{i-1,j}$, $S_{ij} = S_{i-1,j}$

($G_{i-1,j}$, $\rho_{i-1,j}$, $S_{i-1,j}$ are known).

(ii) Obtain a solution for h:

It is assumed that properties vary linearly between stations.

In Eq. (3.16) of C_- characteristic direction, we have

$$\left(\overline{\frac{G}{\rho} - a}\right)_{ij,-} = \frac{1}{2}\left[\left(\frac{G}{\rho} - a\right)_{ij} + \left(\frac{G}{\rho} - a\right)_-\right]$$

$$= \frac{1}{2}\left[\left(\frac{G}{\rho}\right)_- + \left(\frac{G}{\rho}\right)_{ij} - (a_{ij} + a_-)\right]$$

$$= \frac{1}{2}\left[\left(\frac{G}{\rho}\right)_- + \left(\frac{G}{\rho}\right)_{ij} - 2\,\bar{a}_{ij,-}\right]$$

where $\bar{a}_{ij,-} = \frac{1}{2}(a_{ij} + a_-)$

Substituting this value of $\left(\overline{\frac{G}{\rho} - a}\right)_{ij,-}$ in Eq. (3.16), we obtain

$$-\frac{h}{\Delta t} = \frac{1}{2}\left[\frac{G_{i-1,j} + \frac{h}{\Delta z}(G_{i-1,j+1} - G_{i-1,j})}{\rho_{i-1,j} + \frac{h}{\Delta z}(\rho_{i-1,j+1} - \rho_{i-1,j})} + \frac{G_{ij}}{\rho_{ij}} - 2\bar{a}_{ij,-}\right]$$

Simplifying,

$$h^2 + \frac{\left[2\rho_{i-1,j} + (G_{i-1,j+1} - G_{i-1,j})\left(\frac{\Delta t}{\Delta z}\right) + (\rho_{i-1,j+1} - \rho_{i-1,j}) \cdot \left(\frac{G_{ij}}{\rho_{ij}} - 2\bar{a}_{ij,-}\right)\left(\frac{\Delta t}{\Delta z}\right)\right]}{\left[2(\rho_{i-1,j+1} - \rho_{i-1,j})/\Delta z\right]} h$$

$$+ \frac{\left[G_{i-1,j}\ \Delta t + \left(\frac{G_{ij}}{\rho_{ij}} - 2\bar{a}_{ij,-}\right)(\rho_{i-1,j})\ \Delta t\right]}{\left[2(\rho_{i-1,j+1} - \rho_{i-1,j})/\ \Delta z\right]} = 0 \qquad (3.24)$$

Solving this quadratic equation for h, we obtain

$$h = \frac{-B \pm \sqrt{B^2 - 4c}}{2} \qquad (3.25)$$

where

$$B = \frac{\left[2\rho_{i-1,j} + (G_{i-1,j+1} - G_{i-1,j})\left(\frac{\Delta t}{\Delta z}\right) + (\rho_{i-1,j+1} - \rho_{i-1,j}) \cdot \left(\frac{G_{ij}}{\rho_{ij}} - 2\bar{a}_{ij,-}\right)\left(\frac{\Delta t}{\Delta z}\right)\right]}{\left[2(\rho_{i-1,j+1} - \rho_{i-1,j})/\Delta z\right]} \qquad (3.26)$$

and

$$C = \frac{\left[G_{i-1,j}\ \Delta t + \left(\frac{G_{ij}}{\rho_{ij}} - 2\bar{a}_{ij}\right)\left(\rho_{i-1,j}\right)\ \Delta t\right]}{\left[2\left(\rho_{i-1,j+1} - \rho_{i-1,j}\right)/\Delta z\right]} \qquad (3.27)$$

h is set equal to the smallest positive root.

(iii) Obtain a solution of k:

In Eq. (3.14) of C_+ characteristic direction, we have

$$\left[\frac{G}{\rho} + a\right]_{ij,+} = \frac{1}{2}\left[\left(\frac{G}{\rho} + a\right)_{ij} + \left(\frac{G}{\rho} + a\right)_{+}\right]$$

$$= \frac{1}{2}\left[\left(\frac{G}{\rho}\right)_{+} + \left(\frac{G}{\rho}\right)_{ij} + \left(a_{ij} + a_{+}\right)\right]$$

$$= \frac{1}{2}\left[\left(\frac{G}{\rho}\right)_{+} + \left(\frac{G}{\rho}\right)_{ij} + 2\bar{a}_{ij,+}\right]$$

where $\bar{a}_{ij,+} = \frac{1}{2}\left[a_{ij} + a_{+}\right]$

Substituting in Eq. (3.14), we obtain

$$k = \frac{1}{2}\left[\frac{G_{i-1,j} + \frac{k}{\Delta z}\left(G_{i-1,j-1} - G_{i-1,j}\right)}{\rho_{i-1,j} + \frac{k}{\Delta z}\left(\rho_{i-1,j-1} - \rho_{i-1,j}\right)} + \frac{G_{ij}}{\rho_{ij}} + 2\bar{a}_{ij,+}\right] \Delta t$$

Simplifying,

$$k^2 + \frac{\left[2\rho_{i-1,j} - (\frac{\Delta t}{\Delta z})(G_{i-1,j-1} - G_{i-1,j}) - (\frac{\Delta t}{\Delta z})(\rho_{i-1,j-1} - \rho_{i-1,j})(\frac{G_{ij}}{\rho_{ij}} + 2\bar{a}_{ij,+})\right]}{\left[2(\rho_{i-1,j-1} - \rho_{i-1,j})/\Delta z\right]}$$

$$- \frac{\left[G_{i-1,j}\ \Delta t + \Delta t(\rho_{i-1,j})(\frac{G_{ij}}{\rho_{ij}} + 2\bar{a}_{ij,+})\right]}{\left[2(\rho_{i-1,j-1} - \rho_{i-1,j})/\Delta z\right]} = 0$$

Solving this quadratic equation for k,

$$k = \frac{-B \pm \sqrt{B^2 - 4c}}{2} \tag{3.28}$$

k is set equal to the smallest positive root,

where

$$B = \frac{\left[2\rho_{i-1,j} - \frac{\Delta t}{\Delta z}(G_{i-1,j-1} - G_{i-1,j}) - \frac{\Delta t}{\Delta z}(\rho_{i-1,j-1} - \rho_{i-1,j}) \cdot (\frac{G_{ij}}{\rho_{ij}} + 2\bar{a}_{ij,+})\right]}{\left[2(\rho_{i-1,j-1} - \rho_{i-1,j})/\Delta z\right]} \tag{3.29}$$

and

$$C = -\frac{\left[G_{i-1,j}\Delta t + \Delta t\ (\rho_{i-1,j})(\frac{G_{ij}}{\rho_{ij}} + 2\bar{a}_{ij,+})\right]}{\left[2(\rho_{i-1,j-1} - \rho_{i-1,j})/\Delta z\right]} \qquad (3.30)$$

(iv) Obtain a solution for w:

In Eq. (3.18) of C_o characteristic direction,

$$\left[\frac{\overline{G}}{\rho}\right]_{ij,p} = \frac{1}{2}\left[(\frac{G}{\rho})_{ij} + (\frac{G}{\rho})_{p}\right]$$

Thus Eq. (3.18) can be written as

$$w = \frac{1}{2}\left[\frac{G_{ij}}{\rho_{ij}} + \frac{G_{i-1,j} + \frac{w}{\Delta z}(G_{i-1,j-1} - G_{i-1,j})}{\rho_{i-1,j} + \frac{w}{\Delta z}(\rho_{i-1,j-1} - \rho_{i-1,j})}\right]\Delta t$$

Simplifying,

$$w^2 + \left[\frac{2\rho_{i-1,j} - (\frac{G_{ij}}{\rho_{ij}})(\rho_{i-1,j-1} - \rho_{i-1,j})(\frac{\Delta t}{\Delta z}) - (\frac{\Delta t}{\Delta z})(G_{i-1,j-1} - G_{i-1,j})}{\left[2(\rho_{i-1,j-1} - \rho_{i-1,j})/\Delta z\right]}\right]w$$

$$- \frac{\left[(\frac{G_{ij}}{\rho_{ij}})(\rho_{i-1,j})\Delta t + G_{i-1,j}\ \Delta t\right]}{\left[2(\rho_{i-1,j-1} - \rho_{i-1,j})/\Delta z\right]} = 0$$

Solving this quadratic equation in w, we obtain

$$w = \frac{-B \pm \sqrt{B^2 - 4c}}{2} \tag{3.31}$$

where

$$B = \frac{\left[2\rho_{i-1,j} - (\frac{\Delta t}{\Delta z})(G_{i-1,j-1} - G_{i-1,j}) - (\frac{G_{ij}}{\rho_{ij}})(\frac{\Delta t}{\Delta z})(\rho_{i-1,j-1} - \rho_{i-1,j})\right]}{\left[2(\rho_{i-1,j-1} - \rho_{i-1,j})/\Delta z\right]} \tag{3.32}$$

and

$$C = - \frac{\left[G_{i-1,j}\Delta t + (\frac{G_{ij}}{\rho_{ij}})(\rho_{i-1,j})\Delta t\right]}{\left[2(\rho_{i-1,j-1} - \rho_{i-1,j})/\Delta z\right]} \tag{3.33}$$

(v) Compute $G_{\pm}$, $\rho_{\pm}$, $S_{\pm}$ and G_p, ρ_p, S_p according to Eqs. (3.21) through (3.23).

(vi) Compute $\overline{G}_{ij,\pm}$, $\overline{\rho}_{ij,\pm}$, $\overline{S}_{ij,\pm}$, $(\overline{\frac{G}{\rho}})_{ij,\pm}$ and $\overline{G}_{ij,p}$, $\overline{\rho}_{ij,p}$, $\overline{S}_{ij,p}$ according to Eqs. (3.19) and (3.20).

(vii) Compute $\overline{a}_{ij,\pm}$ and $\overline{a}_{ij,p}$ using $\overline{\rho}_{ij,\pm}$, $\overline{S}_{ij,\pm}$ and $\overline{\rho}_{ij,p}$, $\overline{S}_{ij,p}$ in Eq. (2.31).

(viii) Compute $(\overline{Q}_t)_{ij,\pm}$, $(\overline{Q}_t)_{ij,p}$ using $\overline{G}_{ij,\pm}$, $\overline{\rho}_{ij,\pm}$, $\overline{a}_{ij,\pm}$ and $\overline{G}_{ij,p}$, $\overline{\rho}_{ij,p}$, $\overline{a}_{ij,p}$ in Eq. (2.6).

(ix) Solve Eq. (3.17) of particle path characteristic C_o for S_{ij}:

$$S_{ij} = S_p + (\overline{Q}_t)_{ij,p}\Delta t \tag{3.34}$$

(x) Compute $\left[\overline{\frac{\rho a}{\gamma}}\right]_{ij,\pm}$ using $\frac{(\bar{\rho}_{ij,\pm})(\bar{a}_{ij,\pm})}{\gamma}$

(xi) Compute $\left[\overline{F_1 - \frac{\rho a Q_t}{\gamma}}\right]_{ij,+}$ from $\bar{G}_{ij,+}$, $\bar{\rho}_{ij,+}$, $\frac{(\bar{\rho}_{ij,+})(\bar{a}_{ij,+})}{\gamma}$, $(\bar{Q}_t)_{ij,+}$.

(xii) Compute $\left[\overline{F_1 + \frac{\rho a Q_t}{\gamma}}\right]_{ij,-}$ from $\bar{G}_{ij,-}$, $\bar{\rho}_{ij,-}$, $\frac{(\bar{\rho}_{ij,-})(\bar{a}_{ij,-})}{\gamma}$, $(\bar{Q}_t)_{ij,-}$

(xiii) Solve Eqs. (3.13) and (3.15) for ρ_{ij}: Subtracting Eq. (3.15) from (3.13) and simplifying, we obtain

$$\rho_{ij} = \frac{X_1 + X_2 + (RRP - RRM)(S_{ij})}{DEN} \tag{3.35}$$

where

$$RRP = \frac{(\bar{\rho}_{ij,+})(\bar{a}_{ij,+})}{\gamma} \tag{3.36}$$

$$RRM = (\bar{\rho}_{ij,-})(\bar{a}_{ij,-}) \tag{3.37}$$

$$DEN = \left(\overline{\frac{G}{\rho} - a}\right)_{ij,+} - \left(\overline{\frac{G}{\rho} + a}\right)_{ij,-} \tag{3.38}$$

$$X_1 = \left(\overline{\frac{G}{\rho} - a}\right)_{ij,+}(\rho_+) - G_+ + \left[\overline{F_1 - \frac{\rho a Q_t}{\gamma}}\right]_{ij,+}\Delta t - (RRP)(S_+) \tag{3.39}$$

and

$$X_2 = -\left(\overline{\frac{G}{\rho} + a}\right)_{ij,-}(\rho_-) + G_- - \left[\overline{F_1 + \frac{\rho a Q_t}{\gamma}}\right]_{ij,-}\Delta t - (RRM)(S_-) \tag{3.40}$$

(xiv) Solve Eq. (3.13) for G_{ij} and return to step (ii):

$$G_{ij} = - X_1 + \left[\frac{G}{\rho} - a\right]_{ij,+} \rho_{ij} - RRP\ (S_{ij}) \qquad (3.41)$$

where X_1 and RRP are given by Eqs. (3.39) and (3.36) respectively.

(xv) Repeat computation until consecutive values of G_{ij}, ρ_{ij}, S_{ij} agree within prescribed limits. The limits utilized in this work were

$\pm 0.0001\ G_{ij}$, $\pm 0.0001\ \rho_{ij}$, $\pm 0.0001\ S_{ij}$

3.3.2 SOLUTION AT INLET STATION

(a) Run Nos. 1 and 2

At inlet ($z = 0$), $G_{i,1}$ and $S_{i,1}$ are known from Eqs. (2.32) and (2.33) respectively and $\rho_{i,1}$ must be computed. Only one characteristic C_- reaches the inlet end of the channel from inside the (t,z) region. The procedure here is basically the same as that for interior stations except that $G_{i,1}$ and $S_{i,1}$ are known, k and w are not needed, and only two equations (3.15) and (3.16) for C_- characteristic are used.

(b) Run Nos. 7 through 11

In this case, $\rho_{i,1}$ and $S_{i,1}$ are known to be constant from Eqs. (2.35), (2.36) and $G_{i,1}$ must be computed.

The procedure here is exactly the same as described above for run nos. 1, 2 except that $\rho_{i,1}$ is known and $G_{i,1}$ is to be computed.

Solving Eq. (3.15) for $G_{i,1}$, we obtain

$$G_{i,1}=G_{-}+\left(\overline{\frac{G}{\rho}+a}\right)_{il,-}(\rho_{i,1}-\rho_{-})+\left(\overline{\frac{\rho a}{\gamma}}\right)_{il,-}(S_{i,1}-S_{-})-\left[\overline{F_1+\frac{\rho a Q_t}{\gamma}}\right]_{il,-}\Delta t=0 \tag{3.42}$$

3.3.3 SOLUTION AT DISCHARGE STATION

(a) Run Nos. 1 and 2

At the discharge end ($z = L$), $\rho_{i,51}$ is known to be constant from Eq. (2.34). The unknowns here are $G_{i,51}$ and $S_{i,51}$. Two characteristics C_+ and the particle path C_o reach the discharge end for increasing t. The method of solution is exactly as described for interior stations except that $\rho_{i,51}$ is known, h is not needed, only the C_+ and C_o characteristic equations (3.13), (3.14), (3.17) and (3.18) are utilized.

(b) Run Nos. 7 through 11

At the discharge end of the channel the pressure $p_{i,51}$ is prescribed according to Eq. (2.38). The unknowns are $G_{i,51}$, $\rho_{i,51}$ and $S_{i,51}$.

The procedure here is as follows:

(i) Set $G_{i,51} = G_{i-1,51}$, $S_{i,51} = S_{i-1,51}$.

(ii) Compute $\rho_{i,51}$ from Eq. (2.9) ($P_{i,51}$ is specified).

(iii) Obtain solutions for k and w from Eqs. (3.28), (3.29), (3.30) and (3.31), (3.32), (3.33).

(iv) Compute G_+, ρ_+, S_+ and G_p, ρ_p, S_p according to Eqs. (3.21), (3.23).

(v) Compute $\bar{G}_{ij,+}$, $\bar{\rho}_{ij,+}$, $\bar{S}_{ij,+}$, $(\overline{\frac{G}{\rho}})_{ij,+}$ and $\bar{G}_{ij,p}$, $\bar{\rho}_{ij,p}$, $\bar{S}_{ij,p}$ according to Eqs. (3.19), (3.20).

(vi) Compute $\bar{a}_{ij,+}$ and $\bar{a}_{ij,p}$ using $\bar{\rho}_{ij,+}$, $\bar{S}_{ij,+}$ and $\bar{\rho}_{ij,p}$, $\bar{S}_{ij,p}$ in Eq. (2.31).

(vii) Compute $(\bar{Q}_t)_{ij,+}$ and $(\bar{Q}_t)_{ij,p}$ using $\bar{G}_{ij,+}$, $\bar{\rho}_{ij,+}$, $\bar{a}_{ij,+}$ and $\bar{G}_{ij,p}$, $\bar{\rho}_{ij,p}$, $\bar{a}_{ij,p}$ in Eq. (2.6).

(viii) Compute $S_{i,51}$ from Eq. (3.34).

(ix) Compute $\rho_{i,51}$ from Eq. (2.9) using value of $S_{i,51}$ from step (viii).

(x) Compute $\left[\overline{\frac{\rho a}{\gamma}}\right]_{ij,+}$ using $\frac{(\bar{\rho}_{ij,+})(\bar{a}_{ij,+})}{\gamma}$.

(xi) Compute $\left[\overline{F_1 - \frac{\rho a Q_t}{\gamma}}\right]_{ij,+}$ from $\bar{G}_{ij,+}$, $\bar{\rho}_{ij,+}$, $\frac{(\bar{\rho}_{ij,+})(\bar{a}_{ij,+})}{\gamma}$, $(\bar{Q}_t)_{ij,+}$.

(xii) Compute $G_{i,51}$ from Eqs. (3.41), (3.39), (3.36) and return to step (iii).

(xiii) Repeat computation until consecutive values of both G and S agree within prescribed limits, i.e., $\pm 0.0001\ G_{i,51}$, $\pm 0.0001\ S_{i,51}$ in the present work.

3.4 COMPUTER STORAGE

It is important to note that the entire computation may be conducted with three computer storage matrices of 2xM only, except for run numbers 7 to 11, for which one more storage matrix of 2xM for P_{ij} is required. Known values of

G, ρ and S are stored in the first rows and computed ones in the second rows. After printing and/or plotting of the computed values they are moved to the first rows where they act as known values while values computed for the end of the next time interval are stored in the second rows, etc.

A print out of the computer program for run no. 1 appears in Appendix B.

CHAPTER 4

RESULTS AND DISCUSSIONS

4.1 RESULTS

Computed results are shown in Figs. 5 through 26 for various run numbers. G vs. z (Figs. 5, 7, 8, 11), ρ vs. z (Fig. 6), deviation of density from steady state, i.e., $[\rho(0,z) - \rho(t,z)]$ vs. z (Figs. 9, 10), and P vs. z (Fig. 12) are plotted at every 20th computed time interval, i.e., at every $20\Delta t = 0.002$ seconds.

Referring to Fig. 5 it is observed that after 0.002 seconds the expansion wave has only moved about 3 ft downstream. Beyond this region the flow is still undisturbed. Only after about 0.008 seconds is the entire field disturbed.

When the first expansion wave reaches the discharge end it is reflected as a compression wave and can be seen moving back upstream in Fig. 5. It takes about 0.008 second further time to travel upstream to the inlet. It causes further attenuation of local flow rates as it moves upstream.

The same waves may be seen in the density plots of Fig. 6. Under initial steady state conditions ($t = 0$) there is an almost constant decrease in density along the channel. As the inlet flow is retarded this density distribution is gradually disturbed and after about 0.008 seconds

the disturbance is reached at the discharge end. The discharge density is held constant according to the boundary condition and the reflected wave can be seen moving toward the inlet. It takes about 0.008 seconds further to arrive at the inlet.

It is of interest that the inlet density at time 0.016 seconds has decreased to 8.9935 lbs/ft^3 corresponding to a pressure of 1997.98 psia or 1.25 psi below the discharge pressure and the inlet mass flow rate is 92 lbs/ft^2 sec.

The G vs. z plots with heat addition (q = 30 Btu/lb sec) are shown in Fig. 7.

Fig. 8 shows plots of G vs. z for fixed intervals of time following initiation of transient. The effect of increasing mass flow rate at the discharge end due to decrease in pressure, is felt further and further upstream as time increases. At about 0.008 seconds the effect has reached the inlet and the mass flow rate begins to increase there. In order to preserve the prescribed boundary conditions of constant density and constant entropy at the inlet, the wave is reflected and is seen arriving at the discharge end between 0.014 and 0.016 seconds. From the discharge end it is reflected again, and so forth.

Figs. 9 and 10 show plots of deviation of density from steady state vs. distance from channel inlet for fixed intervals of time following initiation of transient. Fig. 11

shows G vs. z plots for the boundary conditions as prescribed in run no. 7. For the same run the P vs. z plots are shown in Fig. 12.

Mass flow rate histories at the inlet and discharge ends of the channel with no heat addition ($q = 0$) are shown in Fig. 13. The inlet flow remains constant at 100 lbs/ft^2 sec until the arrival of first expansion wave at $t \sim 8$ milliseconds. Thereafter, the flow rate begins to increase. It increases to about 4050 lbs/ft^2 sec and then steadies out at $\sim$4025 lbs/ft^2 sec, $t \sim 86$ milliseconds. At the discharge end, the flow rate starts increasing at $t = 0$ and finally becomes steady at $\sim$4025 lbs/ft^2 sec.

Figs. 14 and 15 show the mass flow rate histories at the inlet and discharge ends of the channel with heat addition ($q = 30$ Btu/lb sec). Fig. 15 is drawn on an expanded scale. At inlet, the flow rate remains constant at 100 lbs/ft^2 sec until the first wave from the discharge end arrives there. After arrival the flow rate starts increasing and finally becomes steady at $\sim$3975 lbs/ft^3 sec, $t \sim 130$ milliseconds. The discharge mass flow rate increases to $\sim$150 lbs/ft^2 sec in 1 millisecond and remains almost constant until the first reflected wave arrives there. Then it begins to increase and finally becomes steady at $\sim$3975 lbs/ft^2 sec.

The time variations of mass flow rates at inlet and outlet ends for various runs and with different heat additions are shown plotted in Figs. 16 through 25.

4.2 DISCUSSION OF RESULTS

As mentioned earlier in Chapter 2, in general, the initial conditions along the line $t = 0$, $0 \leq z \leq L$, determine the solution ρ, G, S completely in the region below the C_+ characteristic through $(t,z) = (0,0)$ and the C_- characteristic through $(t,z) = (0,L)$. For the present case (Figs. 5, 6 and 7), the initial conditions are of steady state and ρ is held constant at the boundary $z = L$. As a result, the steady state conditions will prevail in the entire flow field below the C_+ characteristic through the origin in Fig. 4 and the boundary $z = L$. The transient effects due to changes at the inlet will be felt only above this C_+ characteristic. The flow conditions change abruptly at the origin of (t-z) plane. A similar abrupt change will occur as the C_+ characteristic through (0,0) or any of its reflections from the discharge end is crossed (ref. 2).

The expansion wave initiated from the inlet end should show up as a sharp break in the G vs. z and ρ vs. z curves for any given value of t. The present method does not trace the wave exactly, but only infers its position by linear interpolation between grid points. As a result, the sharp break becomes "smeared out" into a smooth shoulder in the curve extending over a range of values of z. This smearing is inherent in the fixed grid method of solution but is not a serious limitation for most cases of practical interest. If the straight portions of the G vs. z curves in Fig. 5 are

extended up to the line G = 100, it can be seen that the line which passes through z = 10 ft, G = 100 lbs/ft^2 sec corresponds to t $\sim$ 0.00825 sec. The theoretical arrival time of this wave can be calculated by the use of Eq. (2.24) of C_+ characteristic. The velocity of this wave is $\sim\frac{G}{\rho}$ + a = $\frac{100}{9.0}$ + 1200 = 1211 ft/sec, giving the time of travel through the channel as $\sim\frac{10}{1211}$ = 0.00825 seconds. The reflected wave from the discharge end is the C_- characteristic and its velocity, from Eq. (2.25), is $\frac{G}{\rho}$ - a $\sim$ $\frac{100}{9}$ - 1200 = -1189 ft/sec. Thus it arrives at the inlet end at t $\sim$ 0.00825 + $\frac{10}{1189}$ = 0.01666 seconds. In Fig. 5 the shoulder in G lines reaches the inlet end between 0.016 and 0.018 seconds. The position of the reflected wave at t = 0.014 seconds may be inferred by extending the two straight parts of the G curve until they intersect at z $\sim$ 3 ft. These two curves for t $\sim$ .00825 seconds and 0.014 seconds are shown as dashed lines in Fig. 5.

In Fig. 7 the expansion wave seems to be arriving at the discharge end between 0.008 and 0.010 seconds. It is reflected as a compression wave and the shoulder in the G lines reaches the inlet between t = .016 and .018 seconds. The effect of heat addition may be noted by comparing Fig. 7 with Fig. 5. As one would expect, the heat addition has the effect of accelerating the flow. We note, for example, that at t =.014 seconds the discharge mass flow rate corresponding to Fig. 7 is $\sim$96.4 lbs/ft^2 sec while in Fig. 5 it is $\sim$94.3 lbs/ft^2 sec.

For the cases represented by Figs. 8 to 25 the region below the C_- characteristic emanating from $(t,z) = (0,L)$ is that of steady state. The transient effects due to changes in flow conditions at the discharge end will be felt only above this C_- curve. The flow conditions change abruptly at $(0,L)$. A similar change will occur as the C_- characteristic through $(0,L)$ or any of its reflections from the inlet is crossed.

The expansion wave initiated from the discharge end should show up as a sharp break in the G vs. z curves for any given value of t, and in the G vs. t curves for any given value of z. As mentioned earlier, in the present method the sharp break becomes "smeared out" into a smooth shoulder in the curve.

Referring to inlet mass flow rate curve of Fig. 13 it is observed that the slope of the curve changes at $t \sim 8$ milliseconds which corresponds to the arrival of the first expansion wave. The slope of the curve shows a decrease at $t \sim 44$ milliseconds which corresponds to the arrival of the last expansion wave. Thereafter the flow rate is increased by the waves arriving at the inlet after reflections from the discharge end. Referring to the discharge flow rate curve it is noticed that there is an almost constant increase in the flow rate upto $t \sim 17$ milliseconds which corresponds to the arrival of the first reflected wave from the inlet end. The slope of the curve

shows a substantial decrease at t ∿ 48 milliseconds corresponding to the arrival time of the last reflected wave. Afterwards the flow rate is increased by the waves arriving at the discharge end after further reflections from the inlet. The waves finally die out. In Fig. 13 it is seen that new steady state is reached at t ∿ 86 milliseconds with G ∿ 4025 lbs/ft^2 sec.

The same waves with heat addition (q = 30 Btu/lb sec) are shown in Figs. 14 and 15. With heat addition, the discharge density being less than without heat, the density drop to the same final value is less. In this case the time taken for this density drop is ∿1 milliseconds as compared to ∿30.5 milliseconds for more drop in the case shown in Fig. 13. From Fig. 15, which is drawn on an enlarged scale, it is seen that there is an almost constant increase in flow rate at the discharge end upto ∿1 millisecond. The flow rate remains almost constant till the arrival of first reflected wave at ∿15 milliseconds; then, it increases. Similarly for the inlet end the flow rate remains constant at 100 lbs/ft^2 sec. upto ∿7.5 milliseconds when the first expansion wave arrives and increases the flow rate. The reflected wave continues to be reflected from each end of the channel in turn until it dies out due to friction. In Fig. 14, it is seen that new steady state is reached at t ∿ 130 milliseconds with G ∿ 3975 lbs/ft^2 sec.

The mass flow rate variations with time when the density drop was a little more than the case explained in Fig. 13 is shown in Fig. 16. It is seen that the waves steady out in a shorter period. The waves shown in Fig. 16 take about 78 milliseconds as against 86 milliseconds of Fig. 13 in steadying out; also the new steady mass flow rate is 4165 lbs/ft^2 sec as against 4025 lbs/ft^2 sec.

The effect of density drop becomes further obvious by comparing Figs. 17 and 18 with Fig. 14. It is seen that a higher density drop yields a quicker steadying out of the waves.

If the pressure is prescribed instead of the density, the resulting curves are shown in Fig. 19 through 25. For small pressure drop of the order of 0.55 percent, the increase in mass flow rates, on arrival of the wave, is gradually diminishing with time due to friction as can be seen in Fig. 20 which has been drawn on an expanded scale. It is further observed that the time taken by the waves to steady out will be large.

The effect of heat addition is seen in Figs. 21, 22 and 23. It is observed that, as in the earlier case, the flow does not reach a steady state condition even at 600 milliseconds (Fig. 21). But if the pressure drop was increased, the flow could be made to reach the new steady state condition in shorter time. This is seen in Figs. 24 and 25 where the pressure drop was kept of the order of 16.7%.

The present computer program of three dependent variables can be made to degenerate back into the two variables program described by Gorman and D'Arcy (2). In the degenerate case, when the entropy is kept constant, it was observed that, by utilizing the velocity of sound relationship of the present program in their program, both the programs give the same results.

4.3 ACCURACY

There is a region in the t, z plane where it is possible to check for computational error by comparing calculated values with known values of the dependent variables. This is the region of steady state conditions. In this region G_{ij}, ρ_{ij} and S_{ij} should be independent of time. Figs. 5 and 6 illustrate that this is so in the present case except for the effect of smearing.

In checking computed mass flow rates with heat addition ($q = 30$ Btu/lb sec) (run no. 2) it is found that the G curves in the steady state region do not approach the $G = 100$ line asymptotically. The portions of the curves above the $G = 100$ line pertain to errors and have not been shown in Fig. 7. From the computed results it is found that the error tends to be a maximum at the discharge end. It was observed that after moving through 80 rows of calculations the maximum error in mass flow rate was 0.73%. Without heat addition (Figs. 5 and 6) the error was negligible. This shows

that the assumption of linear variation of properties between stations is not that good as was in the case of without heat addition.

By simply reducing the time interval to one-half size and doubling the number of station intervals the network grid can be cut in half. This of course requires four times as much computer time. It was found in a trial run that by making these changes the error of 0.73% was reduced to less than 0.3%.

In the case of discharge rupture, represented by run nos. 3 through 11, the discharge end boundary conditions were such that the flow was finally reached a new steady state. This new steady state mass flow rate can be utilized for a steady state solution for ρ and S. Such computations were carried out for run no. 6. Utilizing the new steady flow rate of 4120 lbs/ft^2 sec (Fig. 17), the steady state solution for ρ and S was obtained. The density plots are shown in Fig. 26. It is observed that the two curves (i) new steady-state, and (ii) steady state solution with new steady state mass flow rate, overlap.

4.4 FINAL REMARKS AND SUGGESTION FOR FURTHER WORK

It is seen that the fixed-grid method is easily programmed and has the outstanding advantage in that it provides flow properties as a function of distance along the

channel for fixed intervals of time. No interpolation between computed points is required. The accuracy of the method is readily checked and the network grid size may be easily adjusted so that a suitable compromise can be reached between accuracy and computer running time.

The method described in this thesis is meant for single phase diabatic transient flows of compressible fluids. However, with suitable modifications it could be extended to include two-phase flows. For further work, it is suggested that this technique be extended to include two-phase flows.

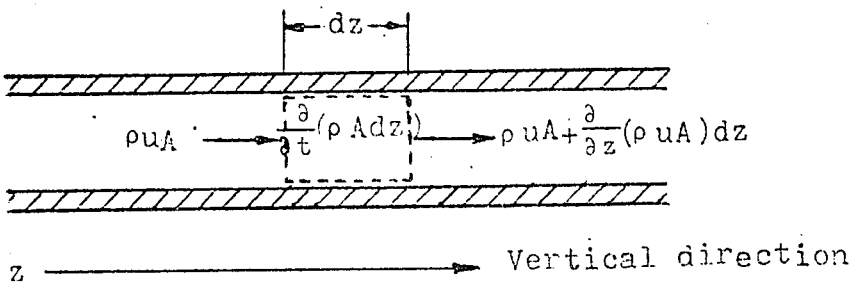

FIG. 1(a): CONTROL VOLUME FOR MASS BALANCE

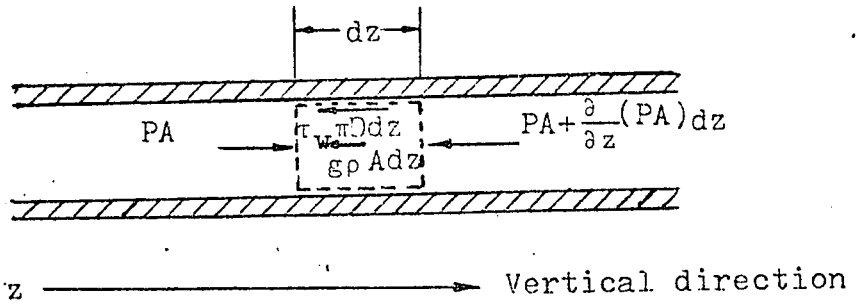

FIG. 1(b): FORCES ACTING ON CONTROL VOLUME ELEMENT

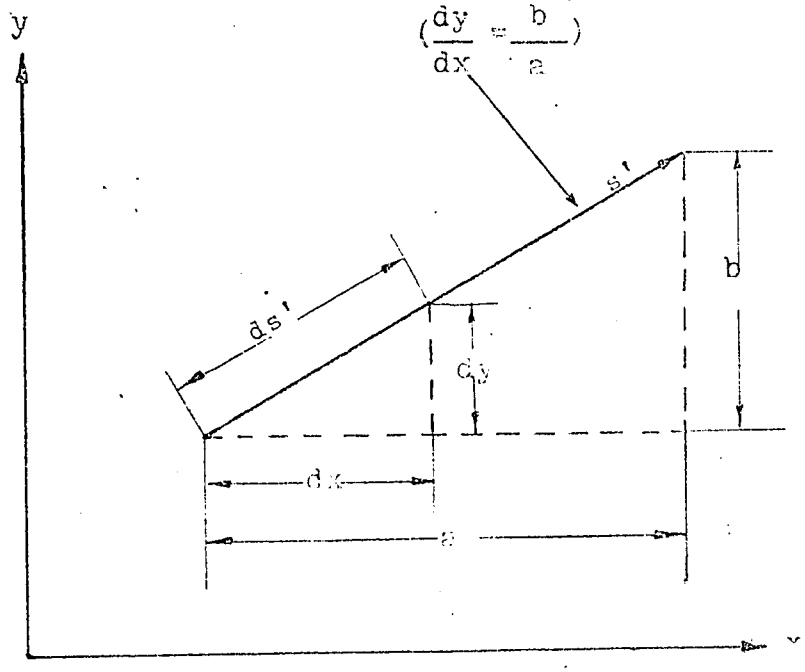

FIG. 2(a): THE s' DIRECTION IN THE (x,y) PLANE

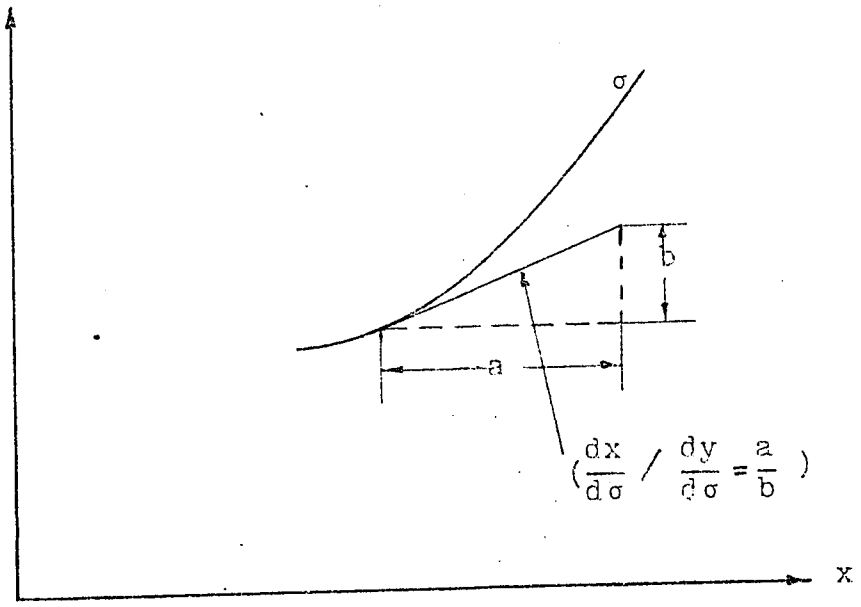

FIG. 2(b): THE σ CURVE IN THE (x,y) PLANE

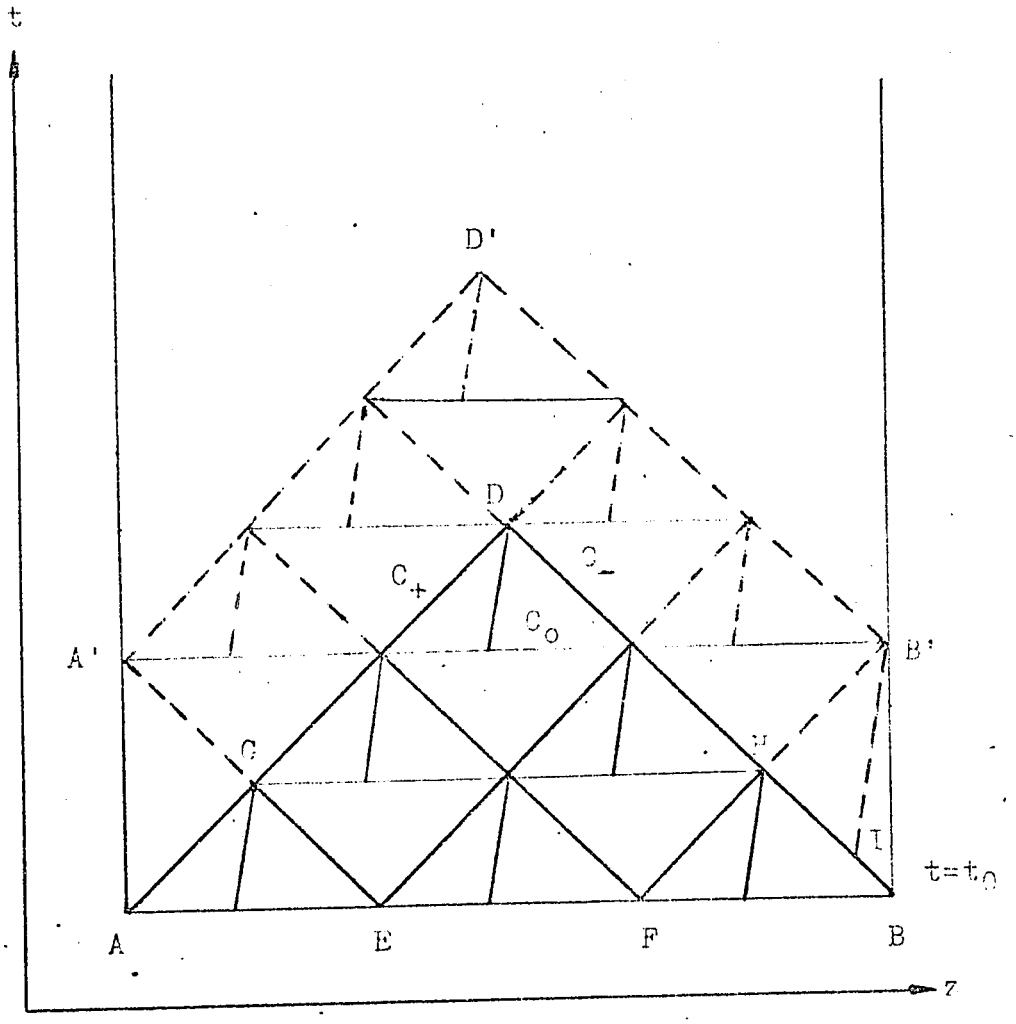

FIG. 3: REGION OF DETERMINED CONDITIONS IN THE (t,z) PLANE

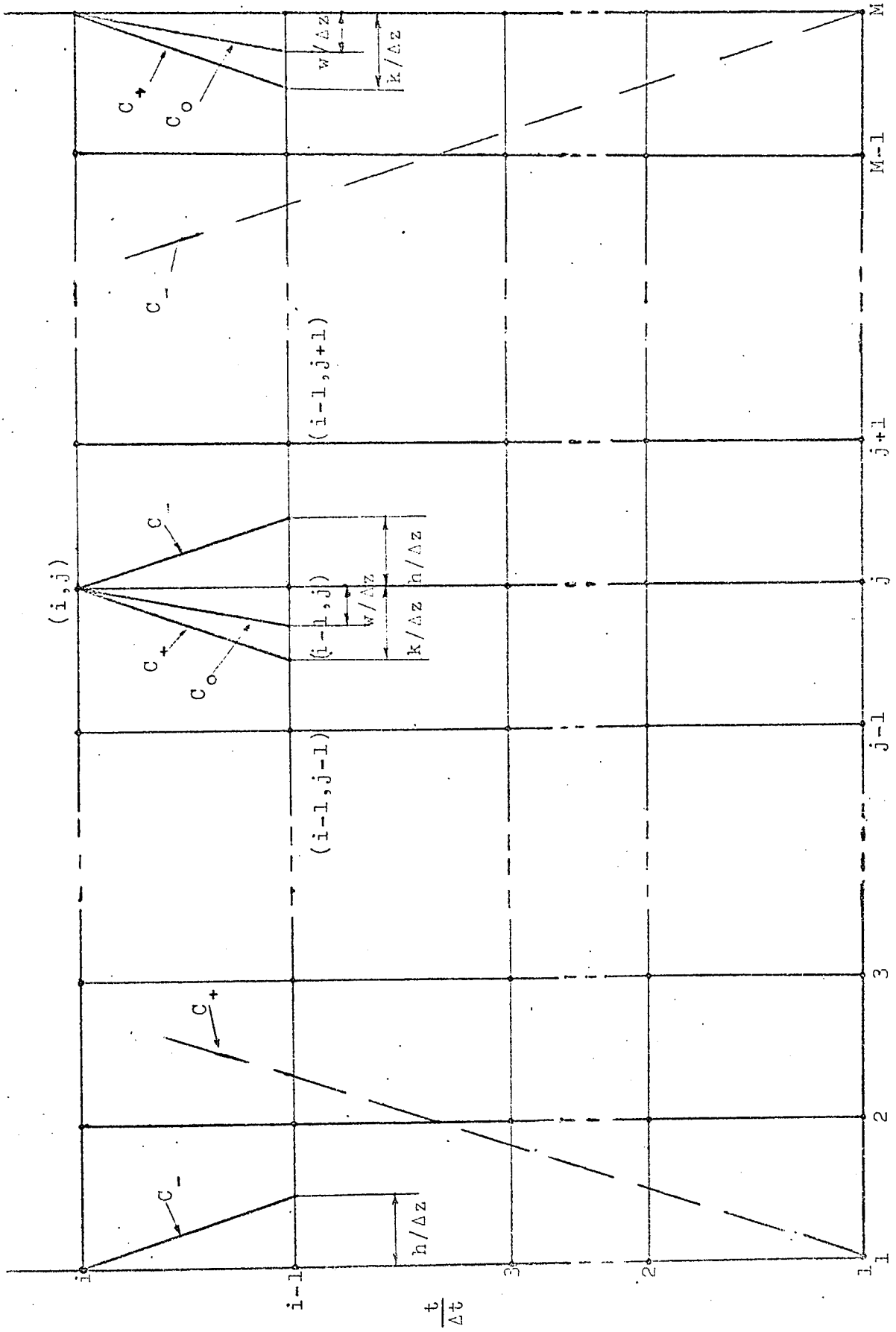

FIG. 4: THE (t,z) PLANE SHOWING THE FIXED GRID AND THE C_+, C_- AND C_o CHARACTERISTIC DIRECTIONS

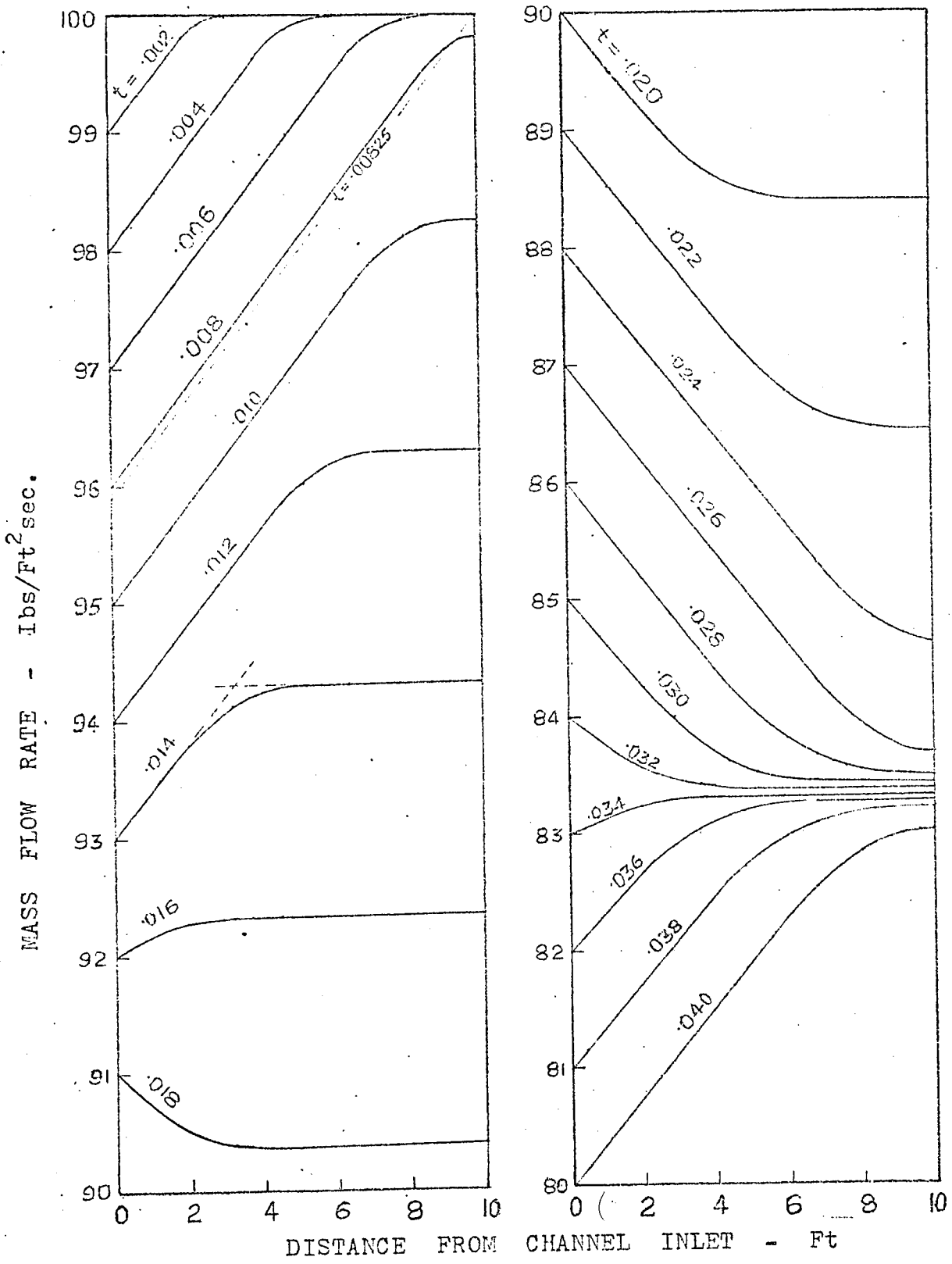

FIG. 5: MASS FLOW RATE VS. DISTANCE FROM CHANNEL INLET (RUN NO. 1)

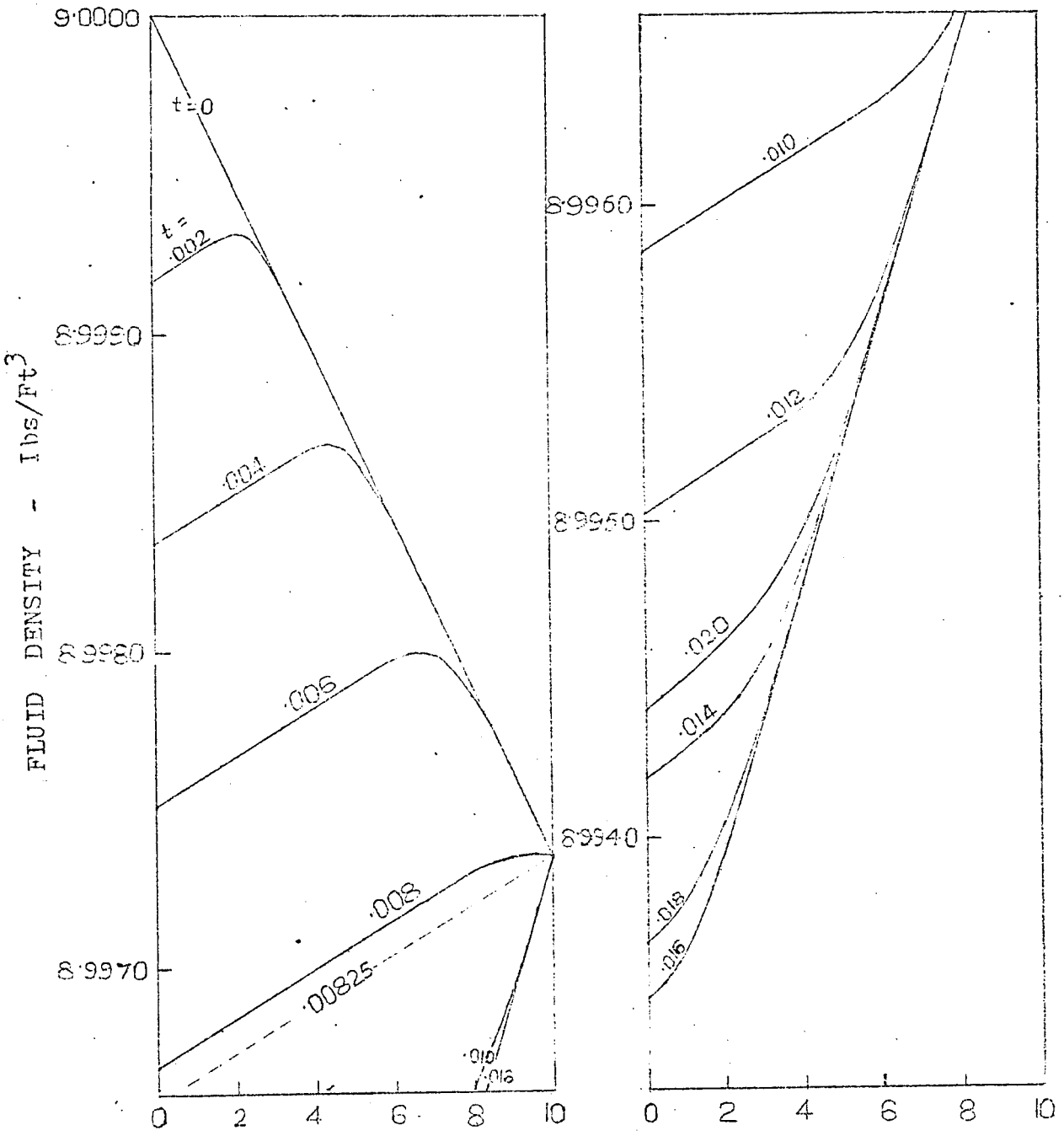

FIG.6 : FLUID DENSITY VS. DISTANCE FROM CHANNEL INLET (RUN NO. 1)

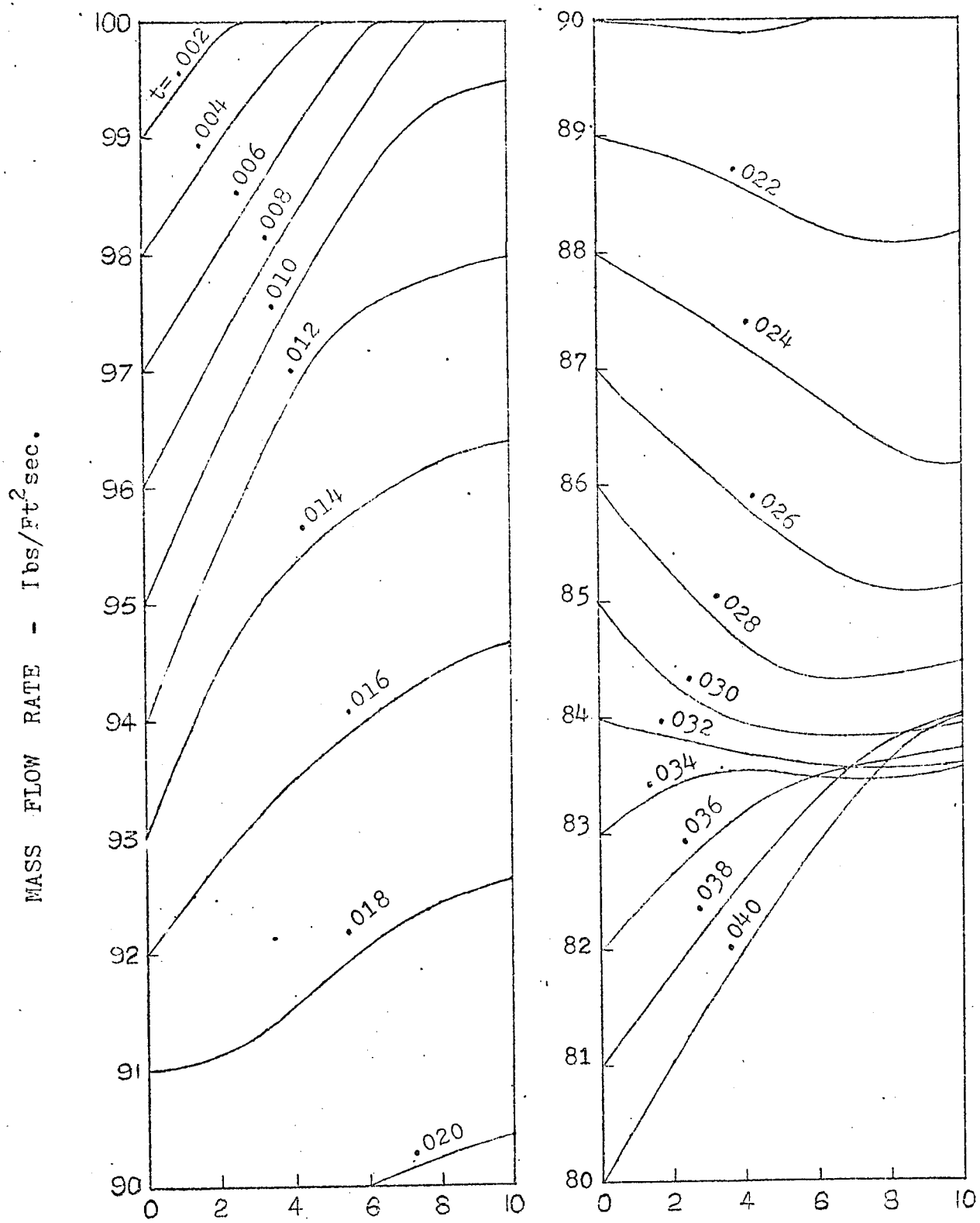

FIG.7 : MASS FLOW RATE VS. DISTANCE FROM CHANNEL INLET (RUN NO.2)

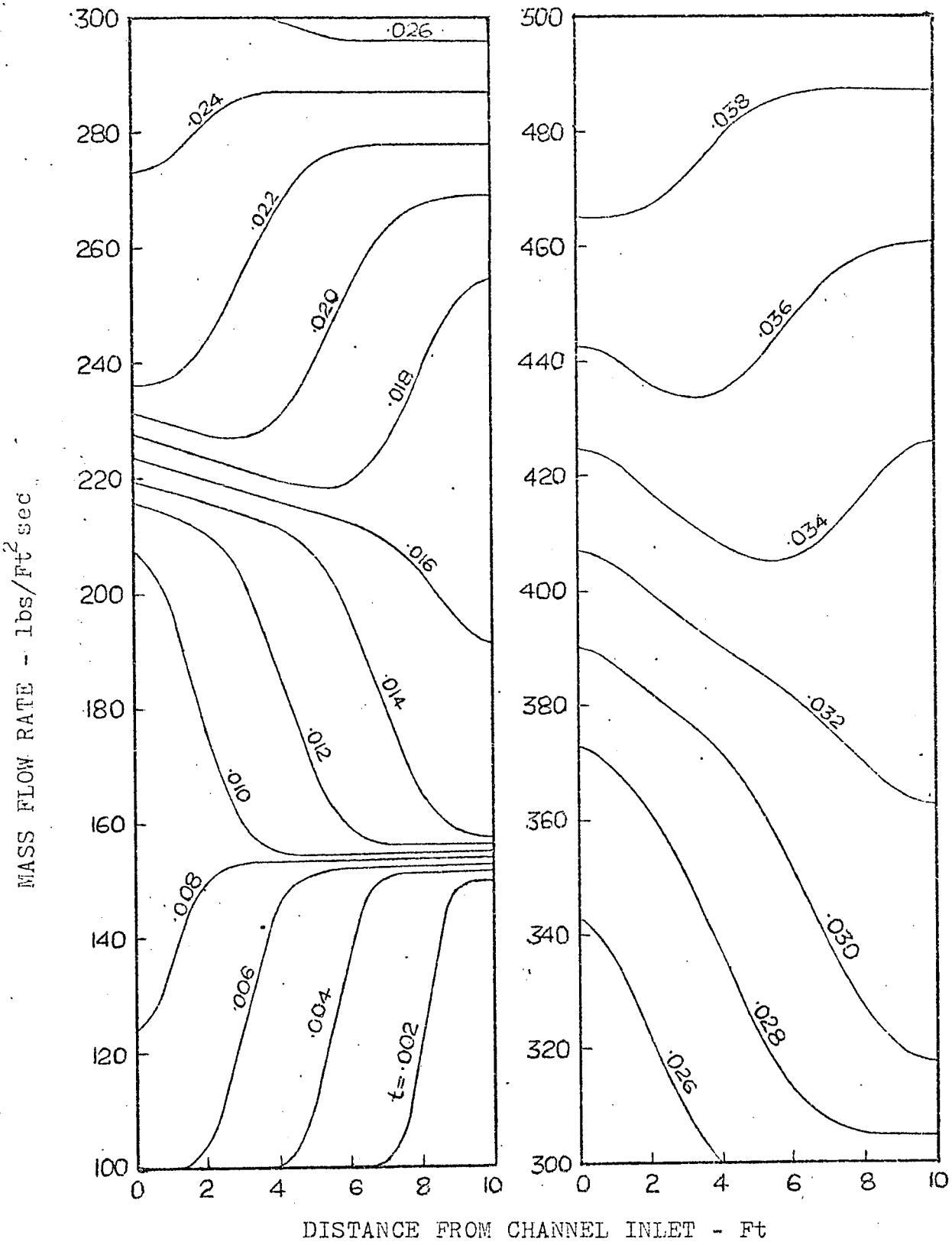

FIG.8: MASS FLOW RATE VS. DISTANCE FROM CHANNEL INLET (RUN NO. 4).

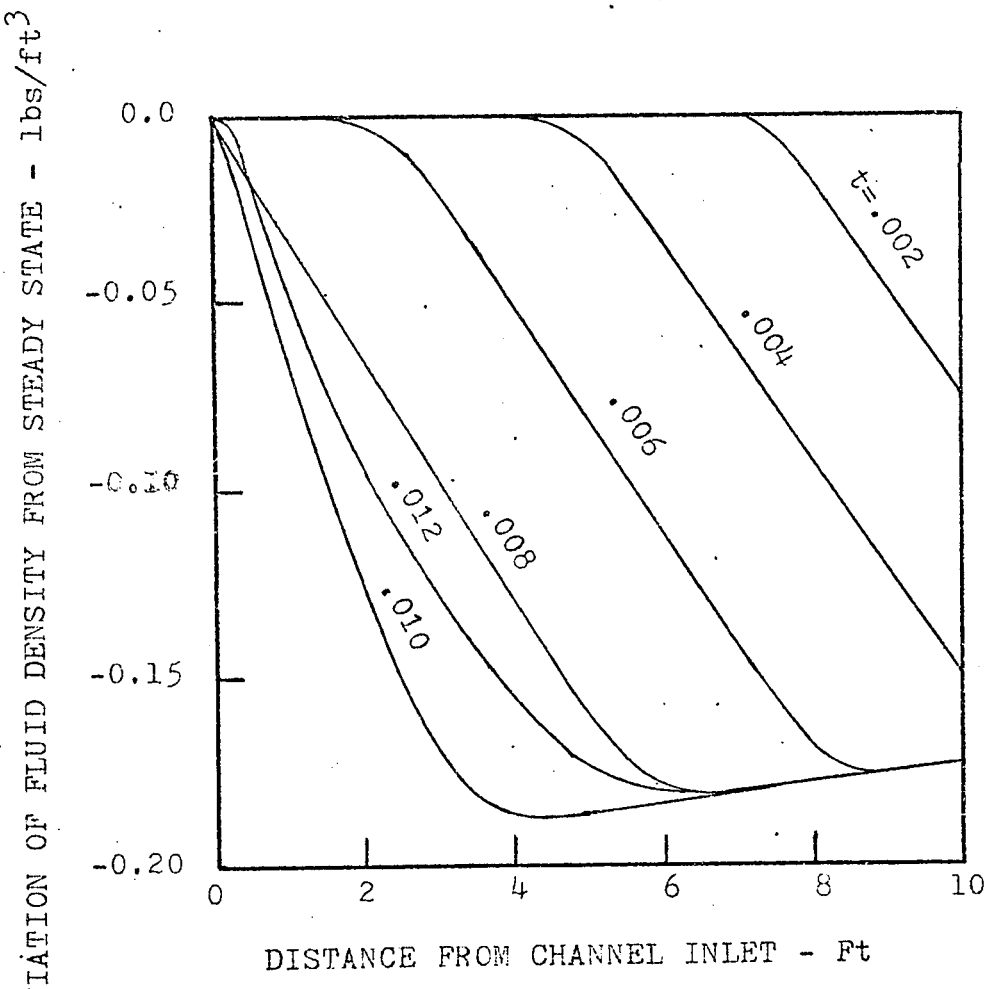

FIG.9 : DEVIATION OF FLUID DENSITY FROM STEADY STATE VS. DISTANCE FROM CHANNEL INLET (RUN NO. 6)

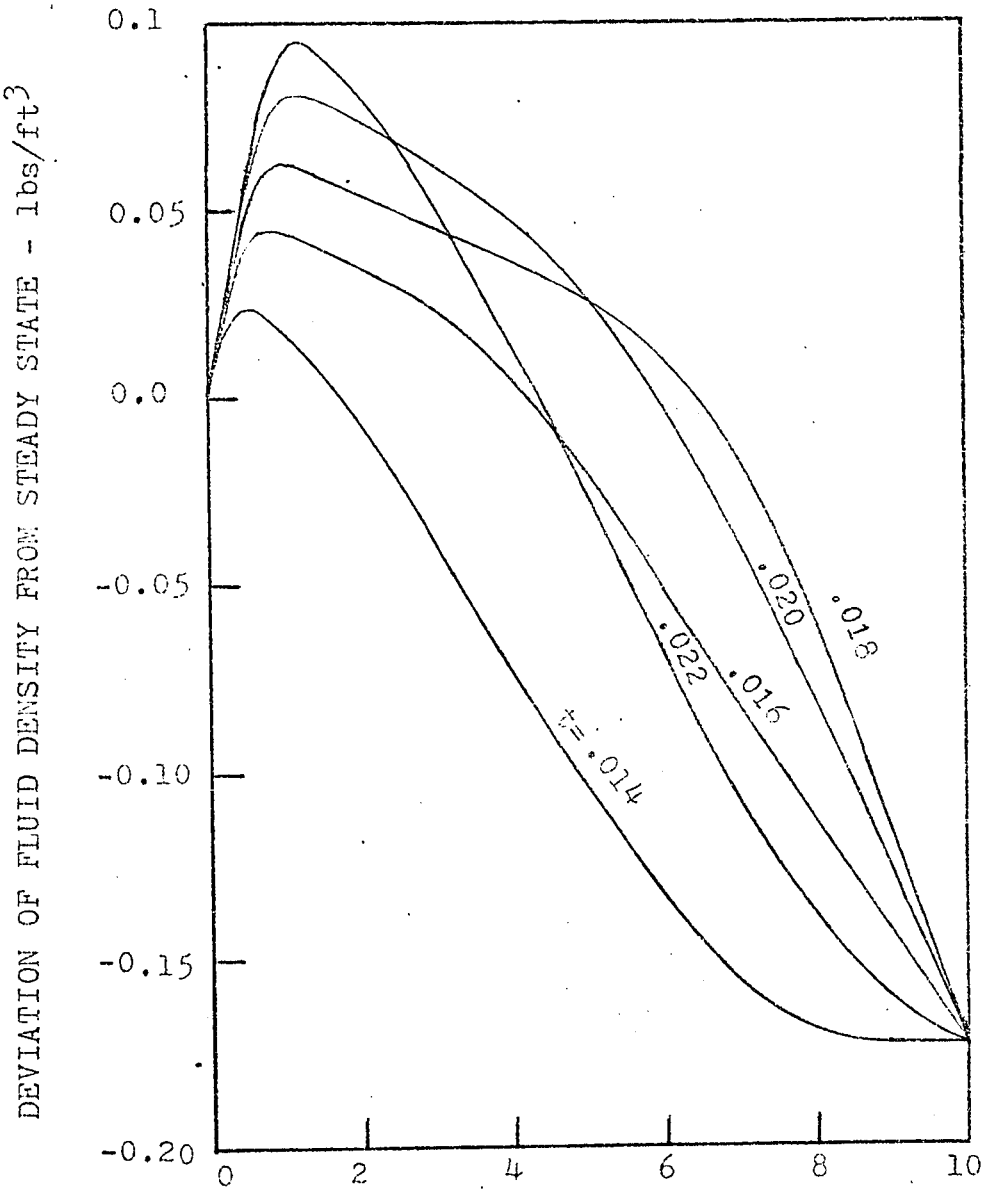

FIG. 10: DEVIATION OF FLUID DENSITY FROM STEADY STATE VS. DISTANCE FROM CHANNEL INLET (RUN NO. 6)

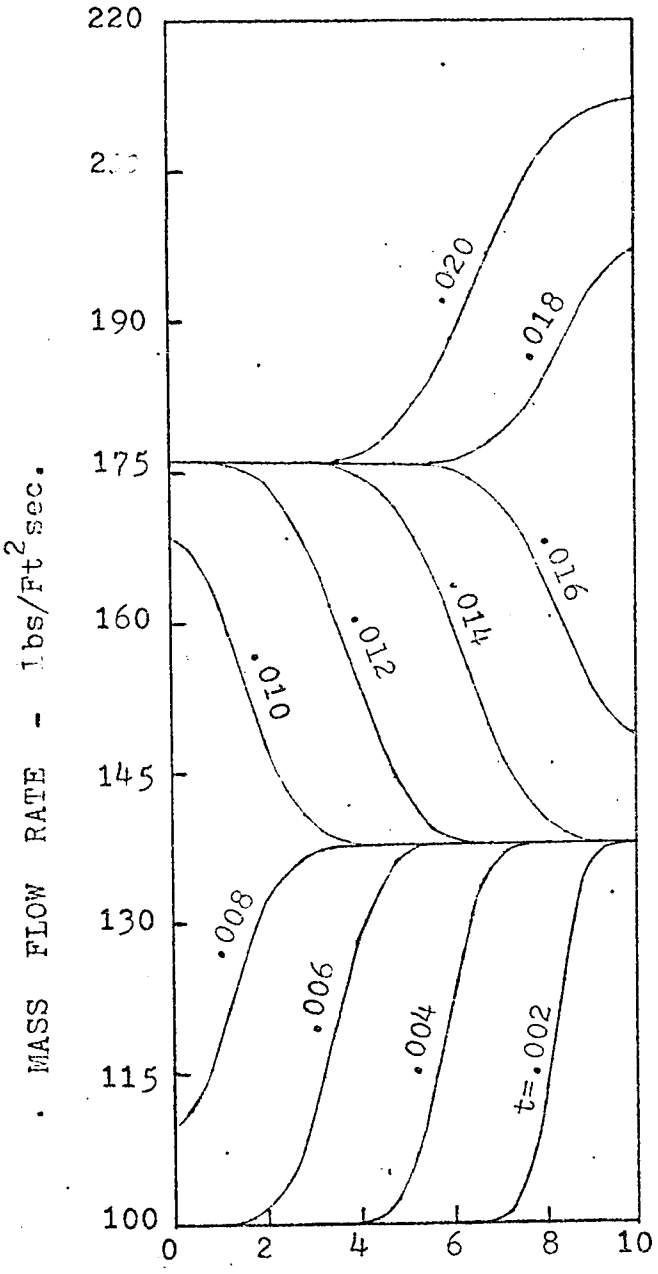

FIG. 11: MASS FLOW RATE VS. DISTANCE FROM CHANNEL INLET (RUN NO. 7)

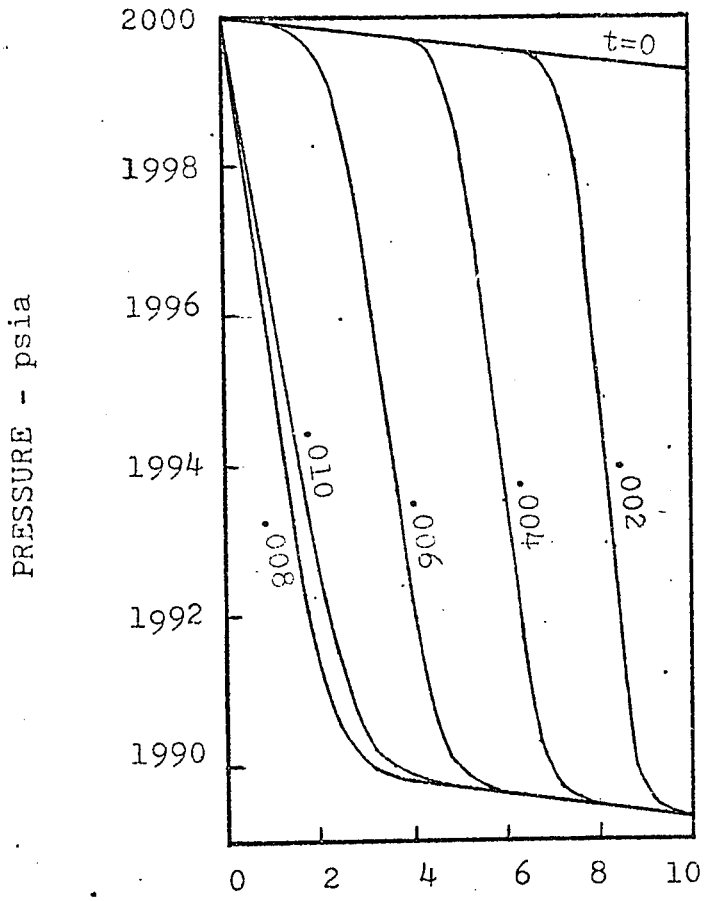

FIG. 12: PRESSURE VS. DISTANCE FROM CHANNEL INLET (RUN NO. 7)

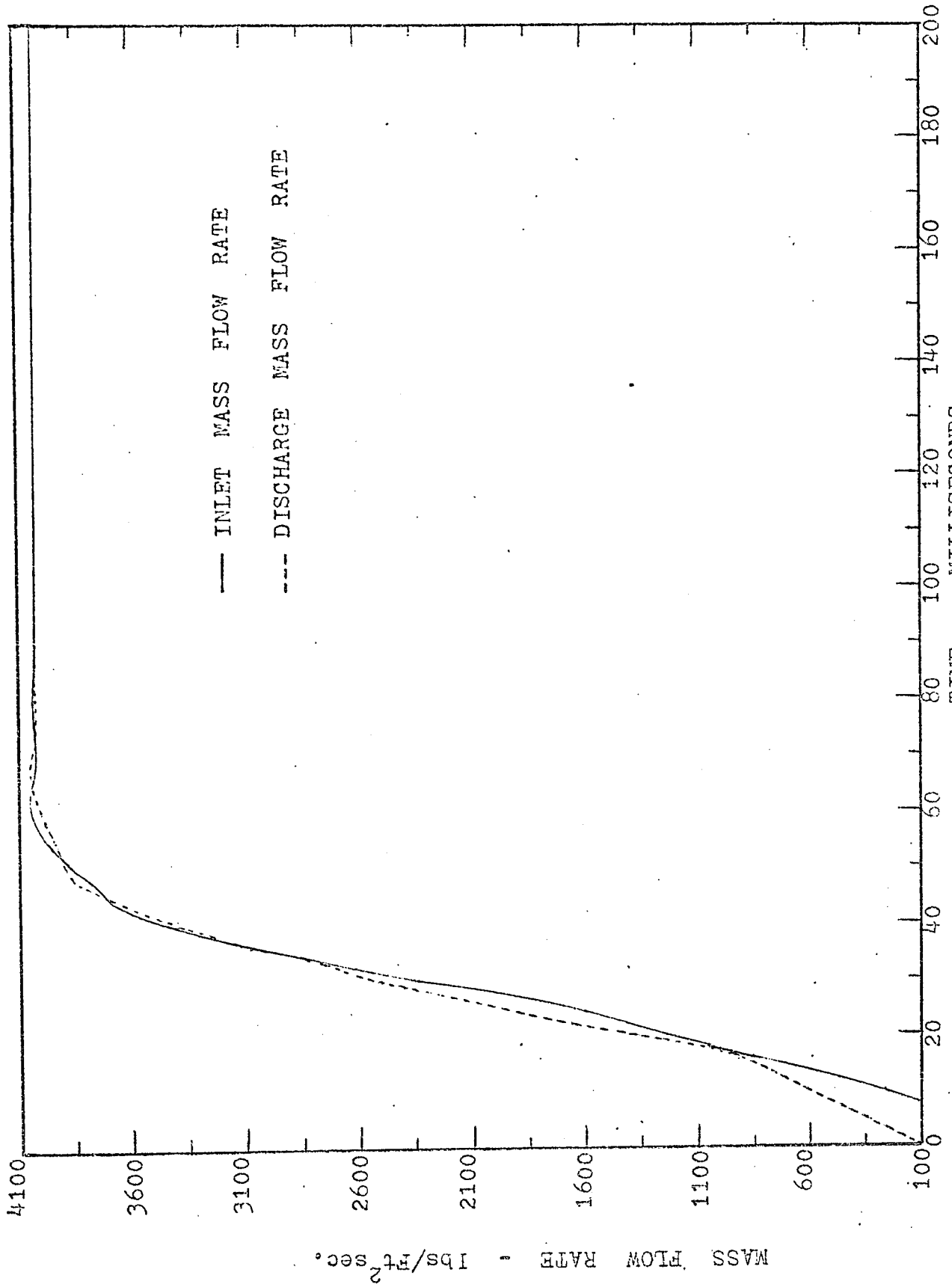

FIG. 13: MASS FLOW RATE VS. TIME (RUN NO. 3)

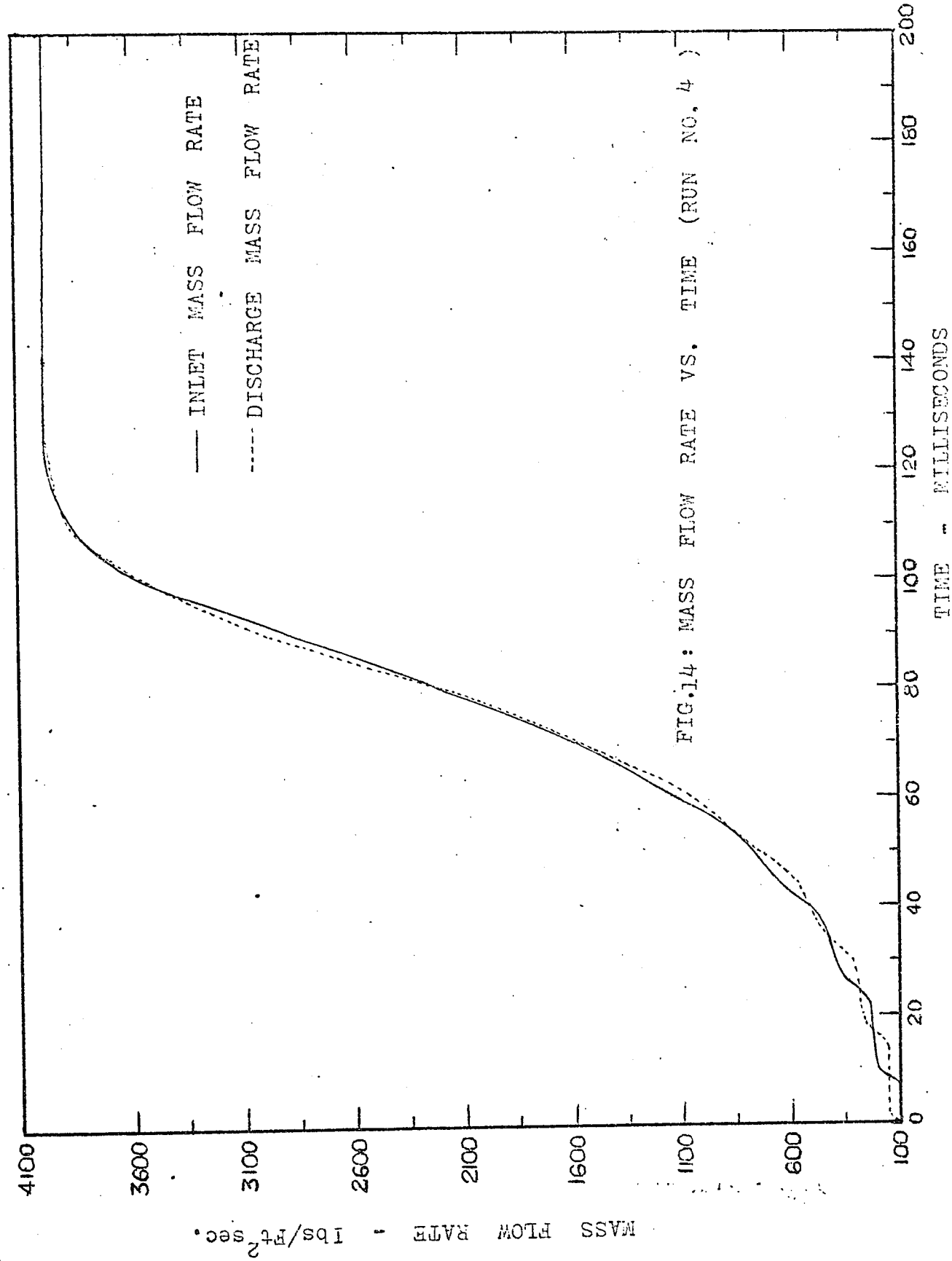

FIG.14: MASS FLOW RATE VS. TIME (RUN NO. 4)

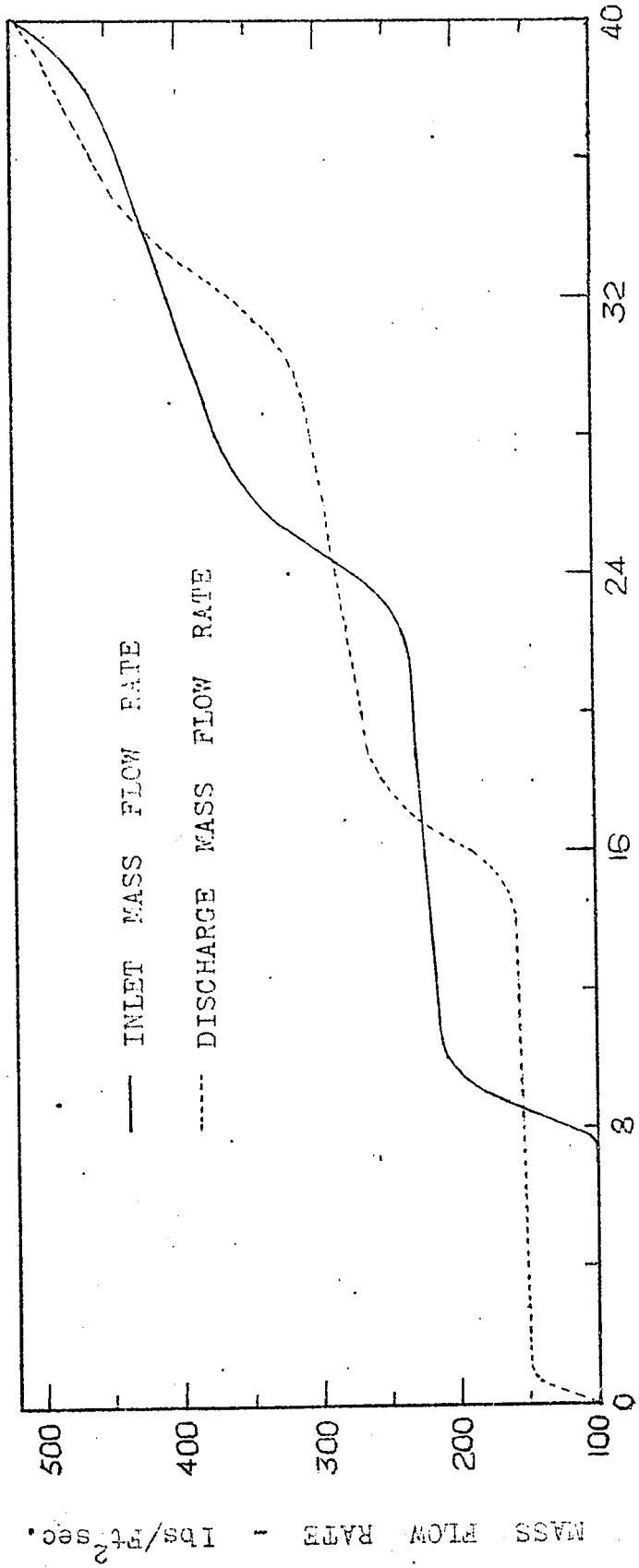

FIG. 15: MASS FLOW RATE VS. TIME (RUN NO. 4)

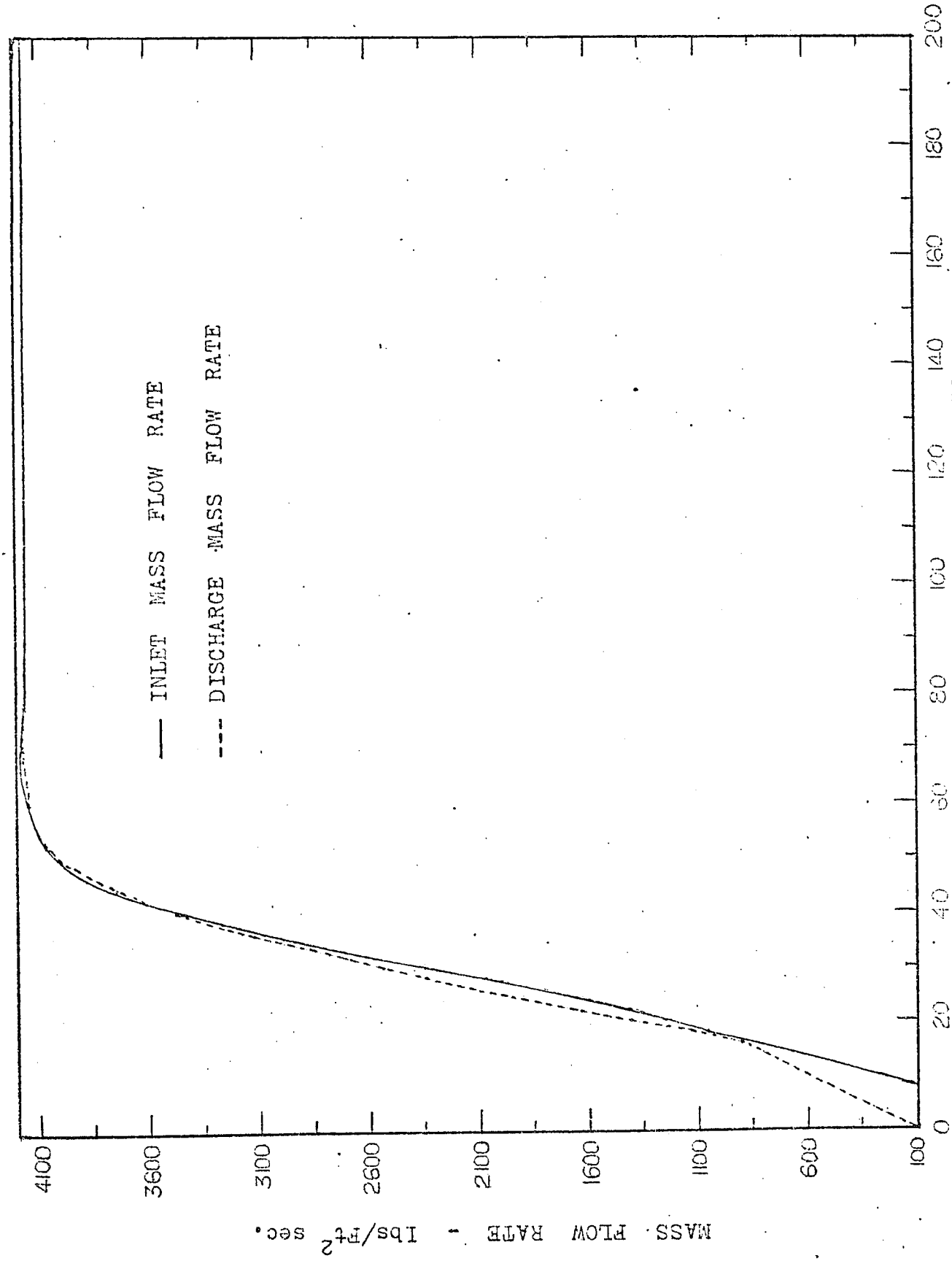

FIG.16: MASS FLOW RATE VS. TIME (RUN NO. 5)

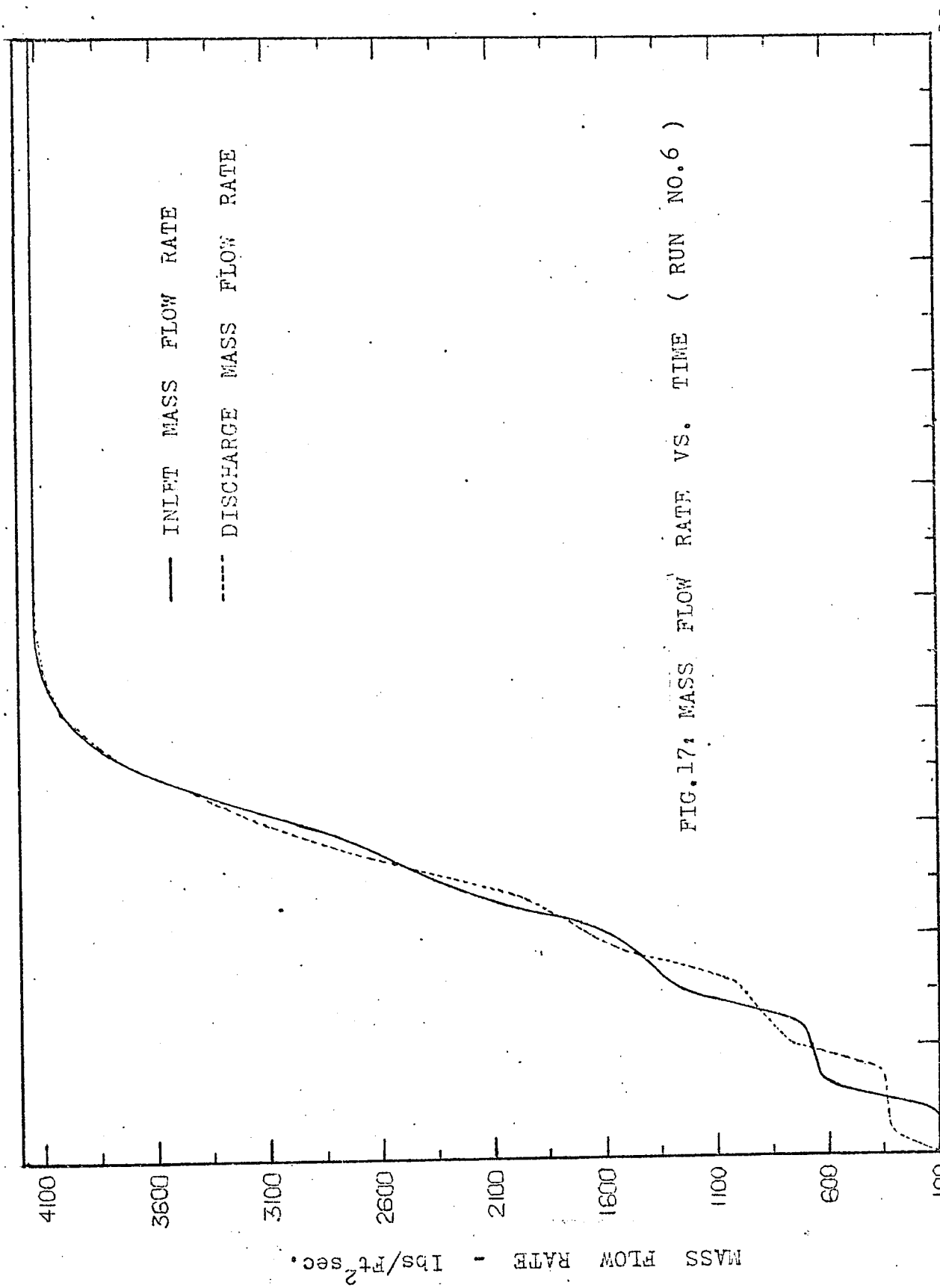

FIG. 17: MASS FLOW RATE VS. TIME (RUN NO. 6)

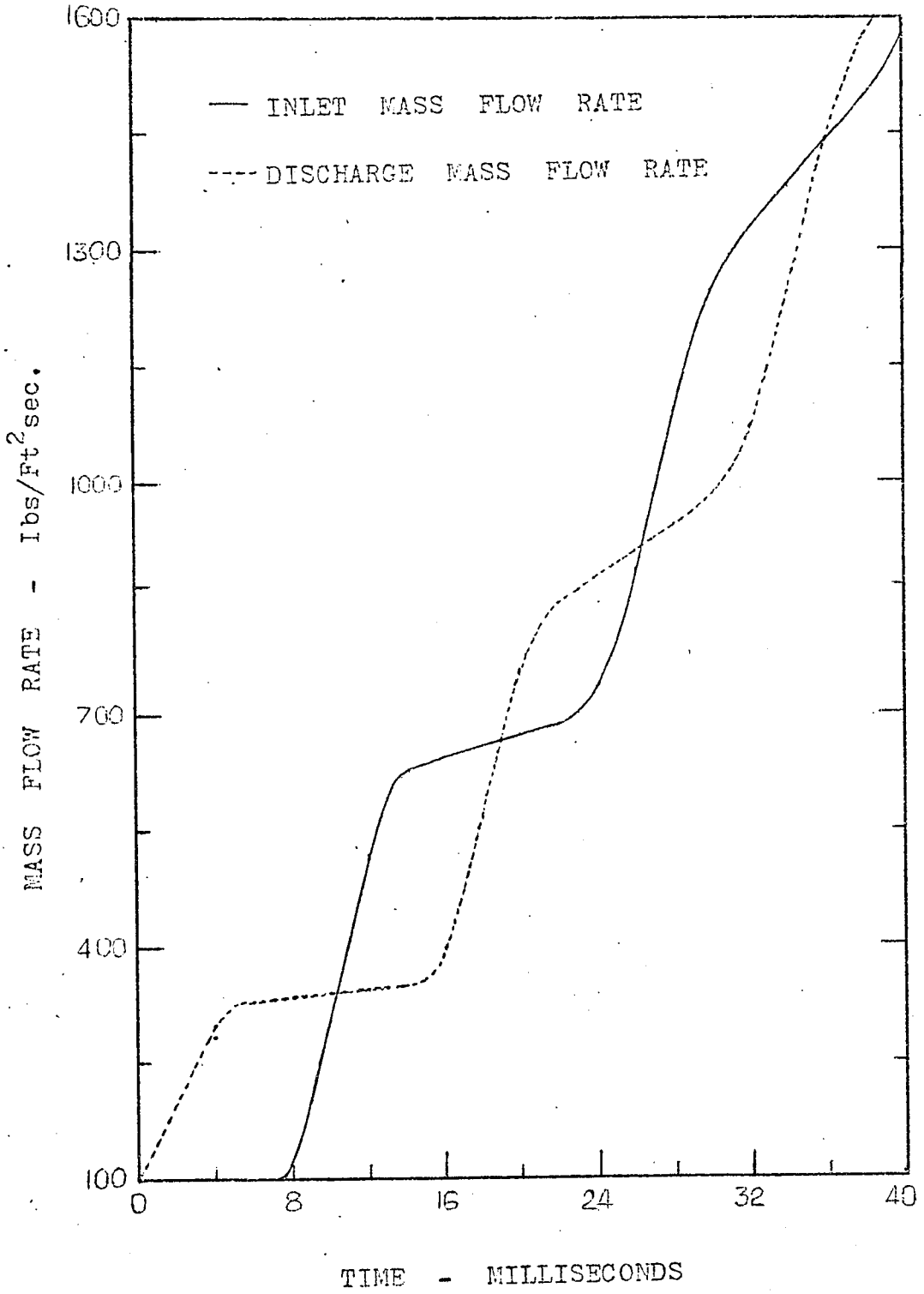

FIG. 18: MASS FLOW RATE VS. TIME (RUN NO. 6)

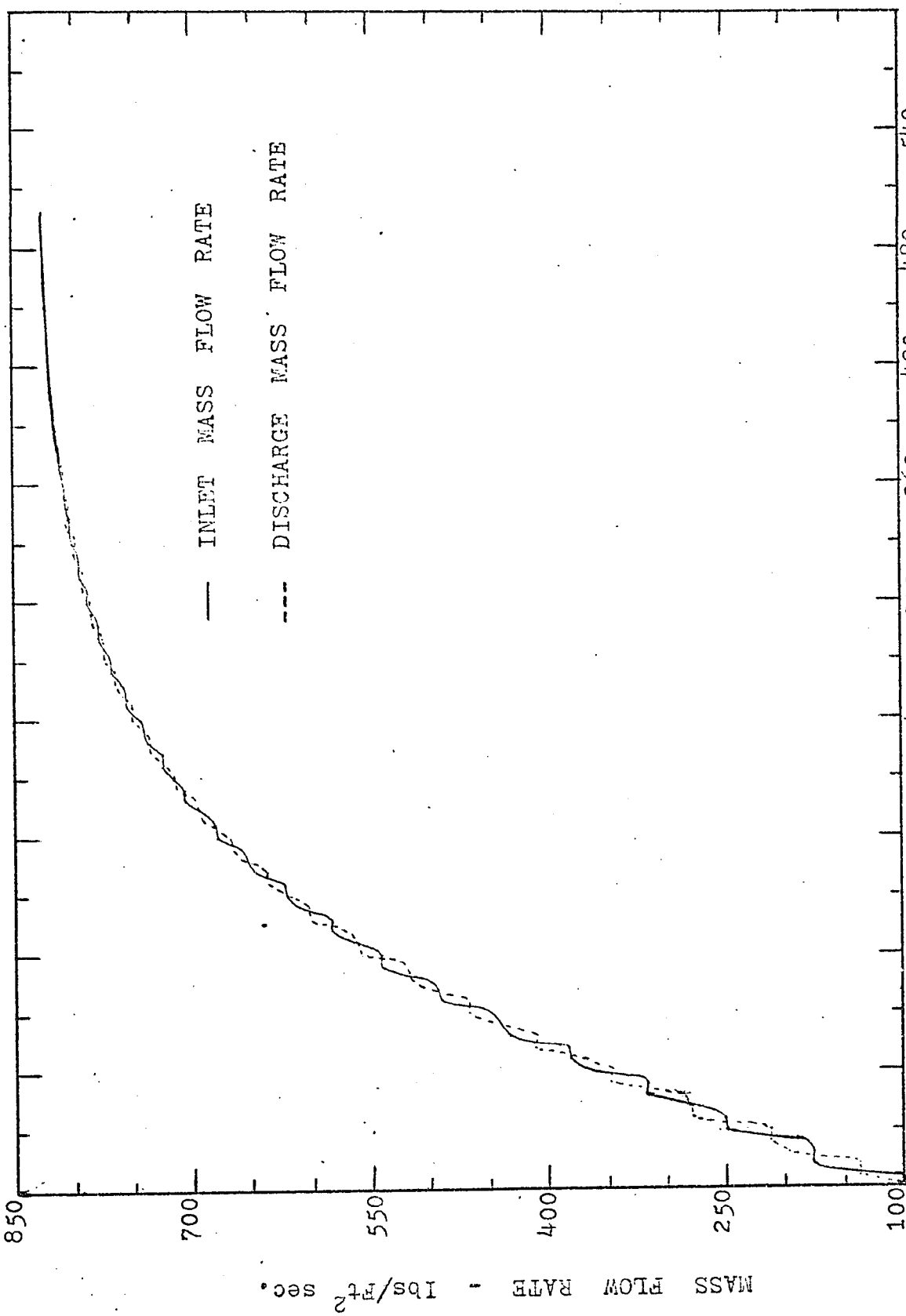

FIG.19: MASS FLOW RATE VS. TIME (RUN NO. 7)

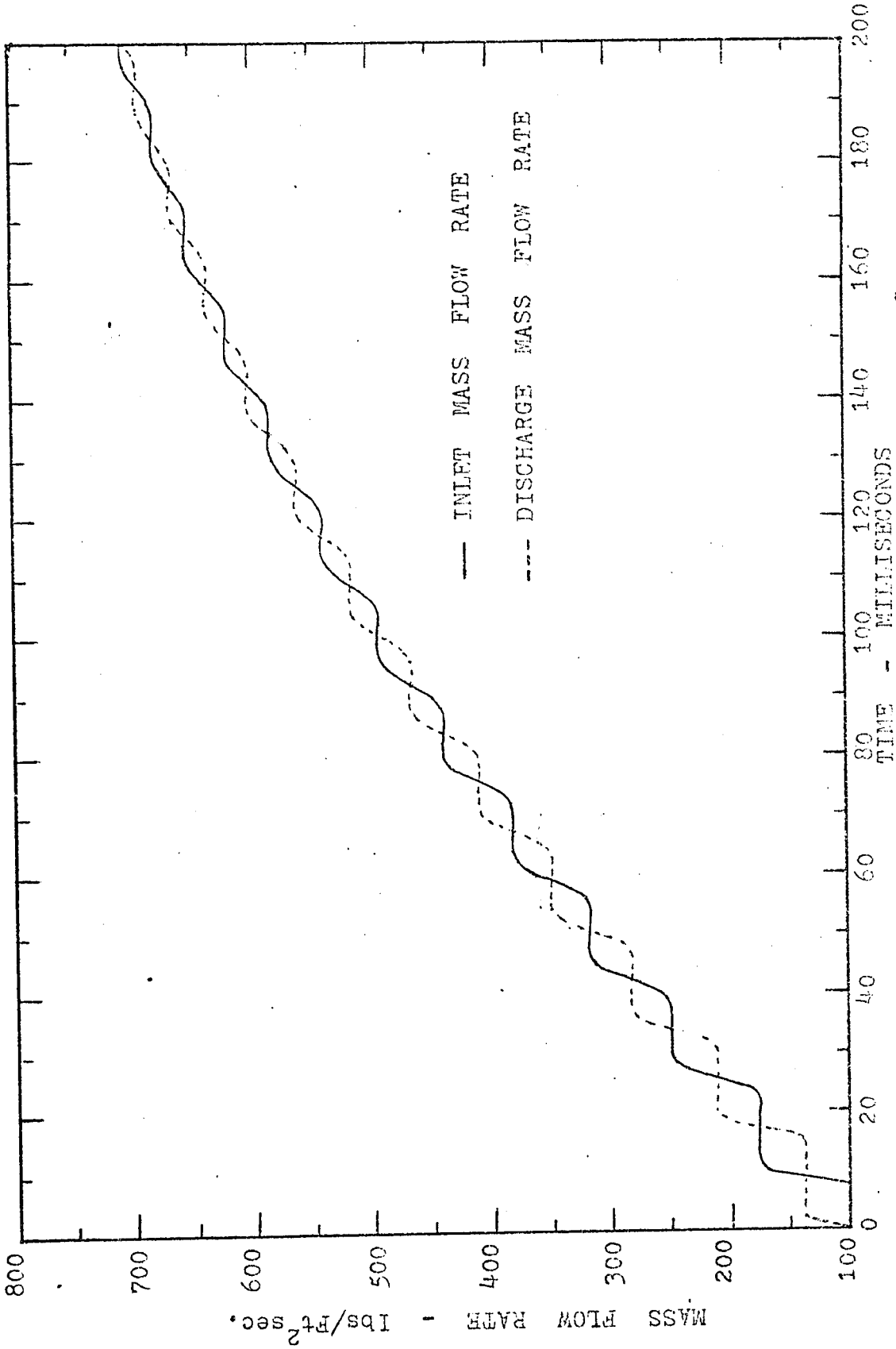

FIG.20: MASS FLOW RATE VS. TIME (RUN NO. 7)

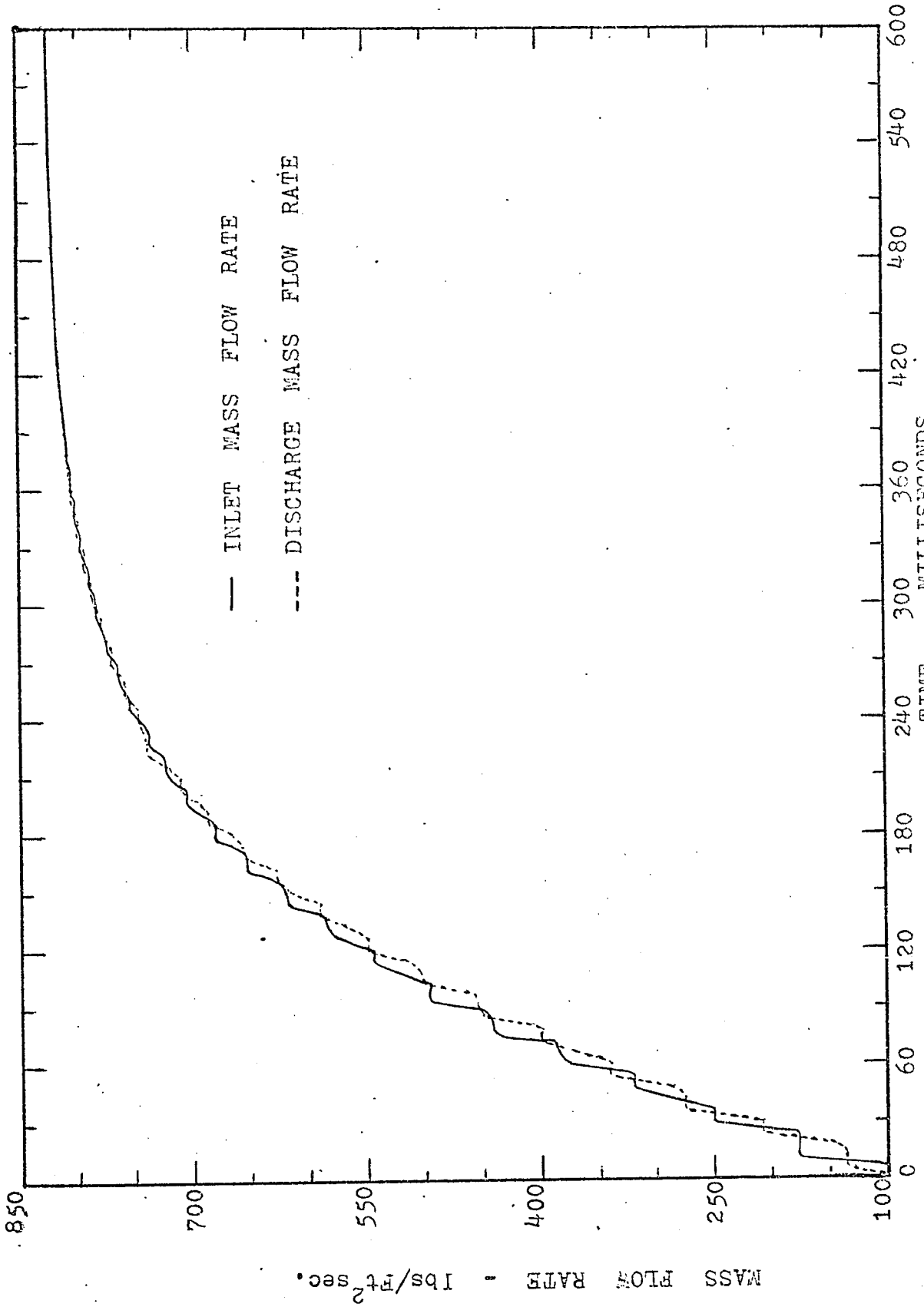

FIG.21: MASS FLOW RATE VS. TIME (RUN NO. 8)

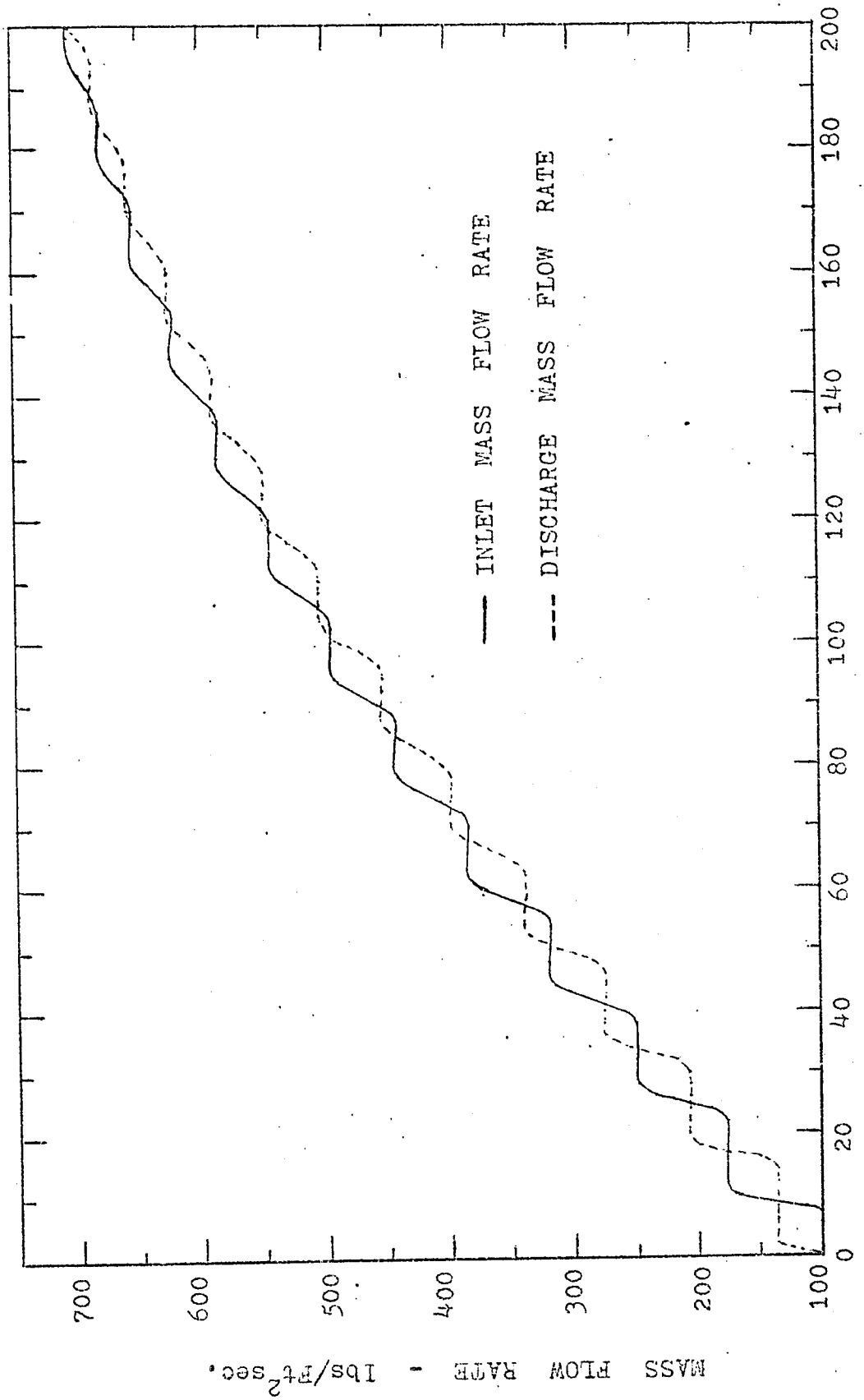

FIG.22: MASS FLOW RATE VS. TIME (RUN NO.8)

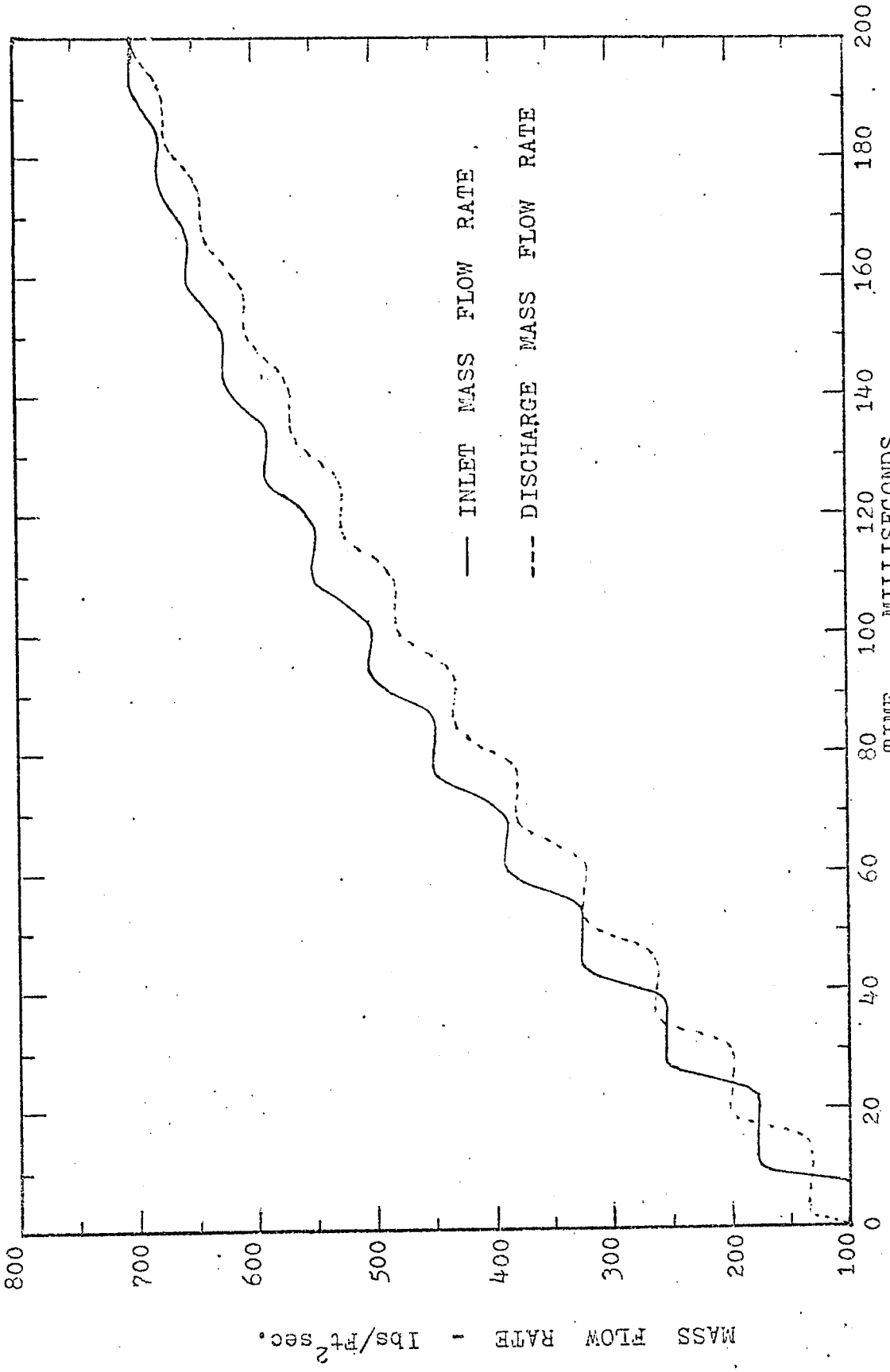

FIG. 23: MASS FLOW RATE VS. TIME (RUN NO. 9)

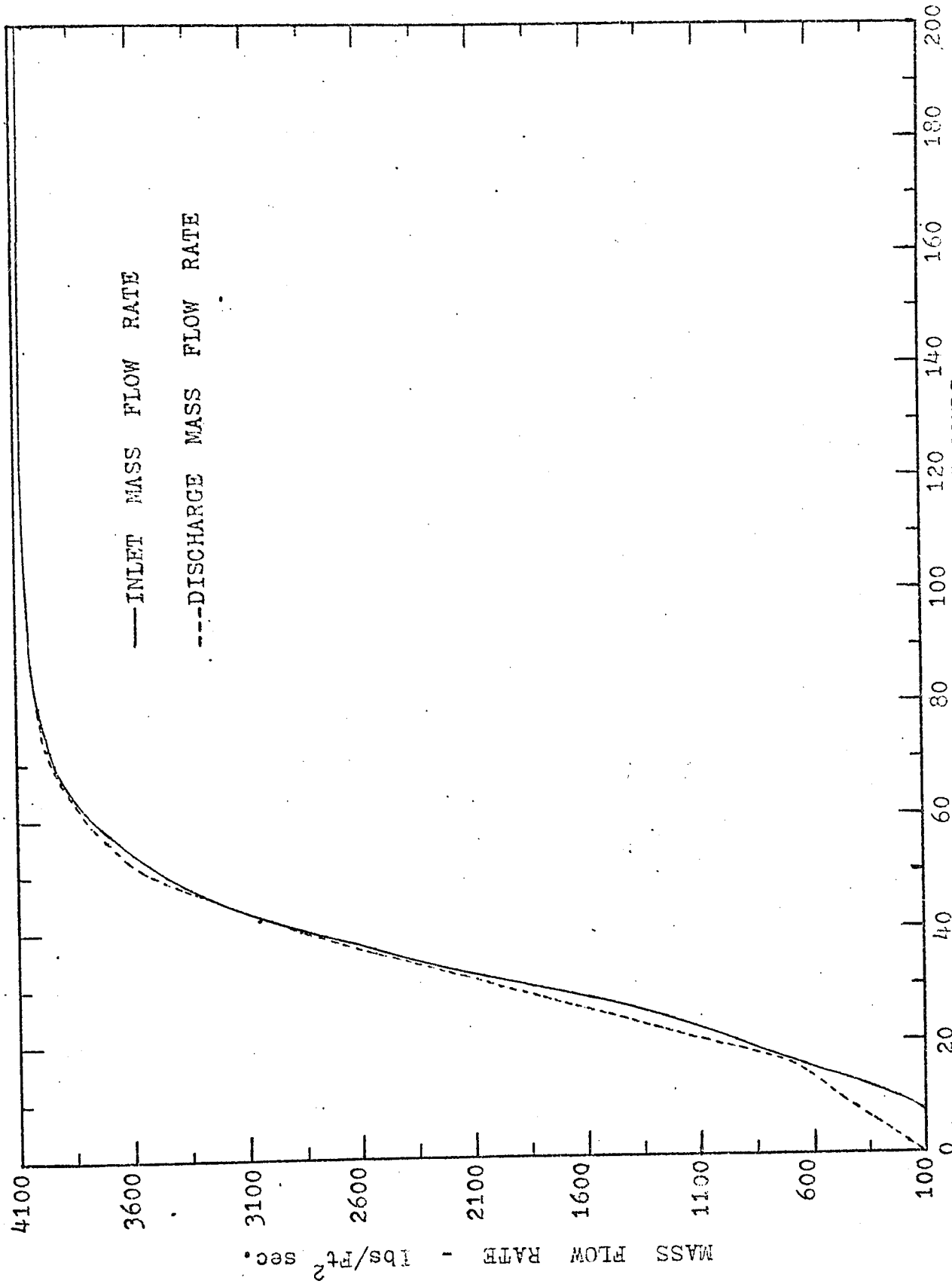

FIG. 24 : MASS FLOW RATE VS. TIME (RUN NO.10)

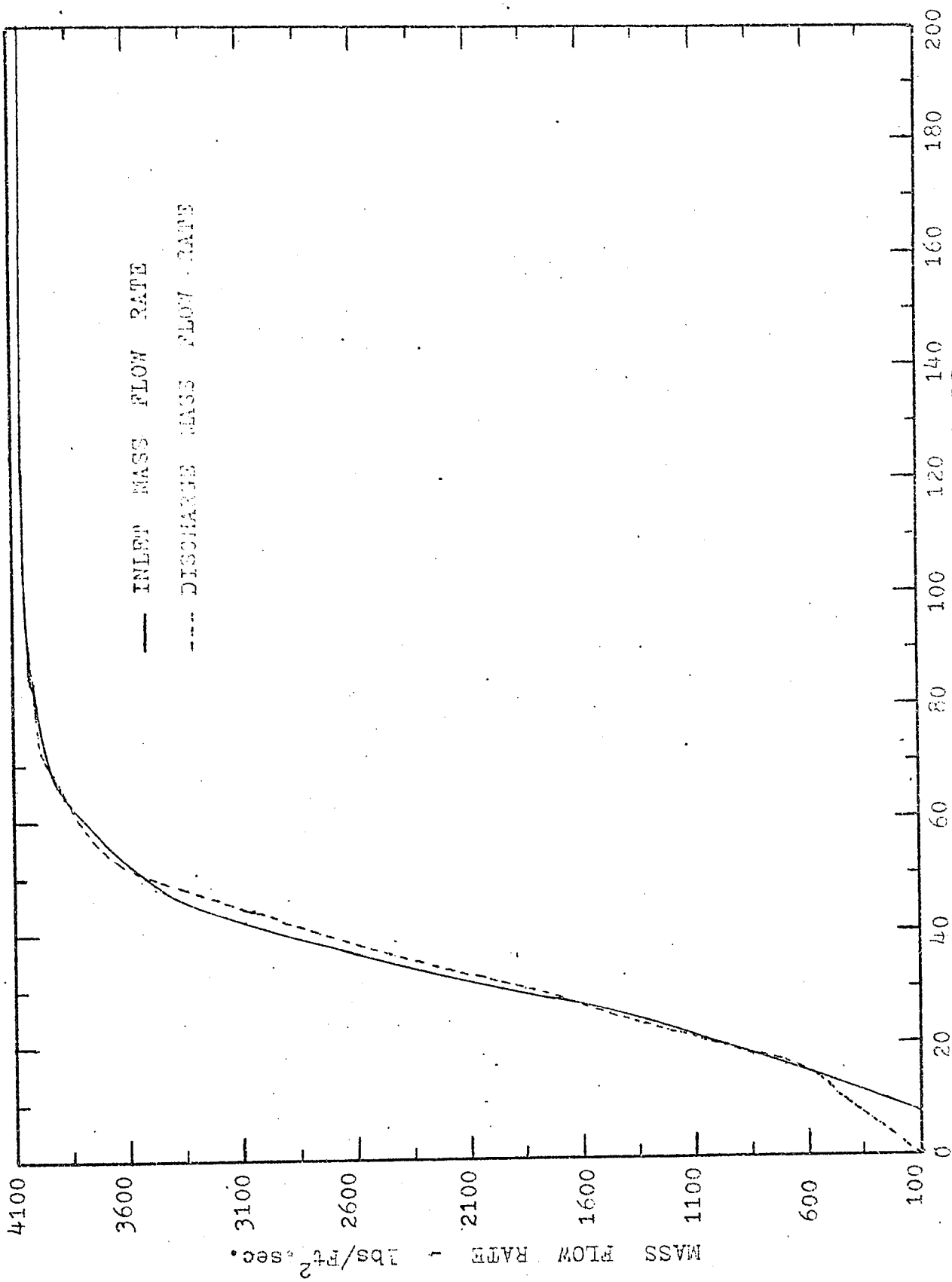

FIG.25: MASS FLOW RATE VS. TIME (RUN NO.11)

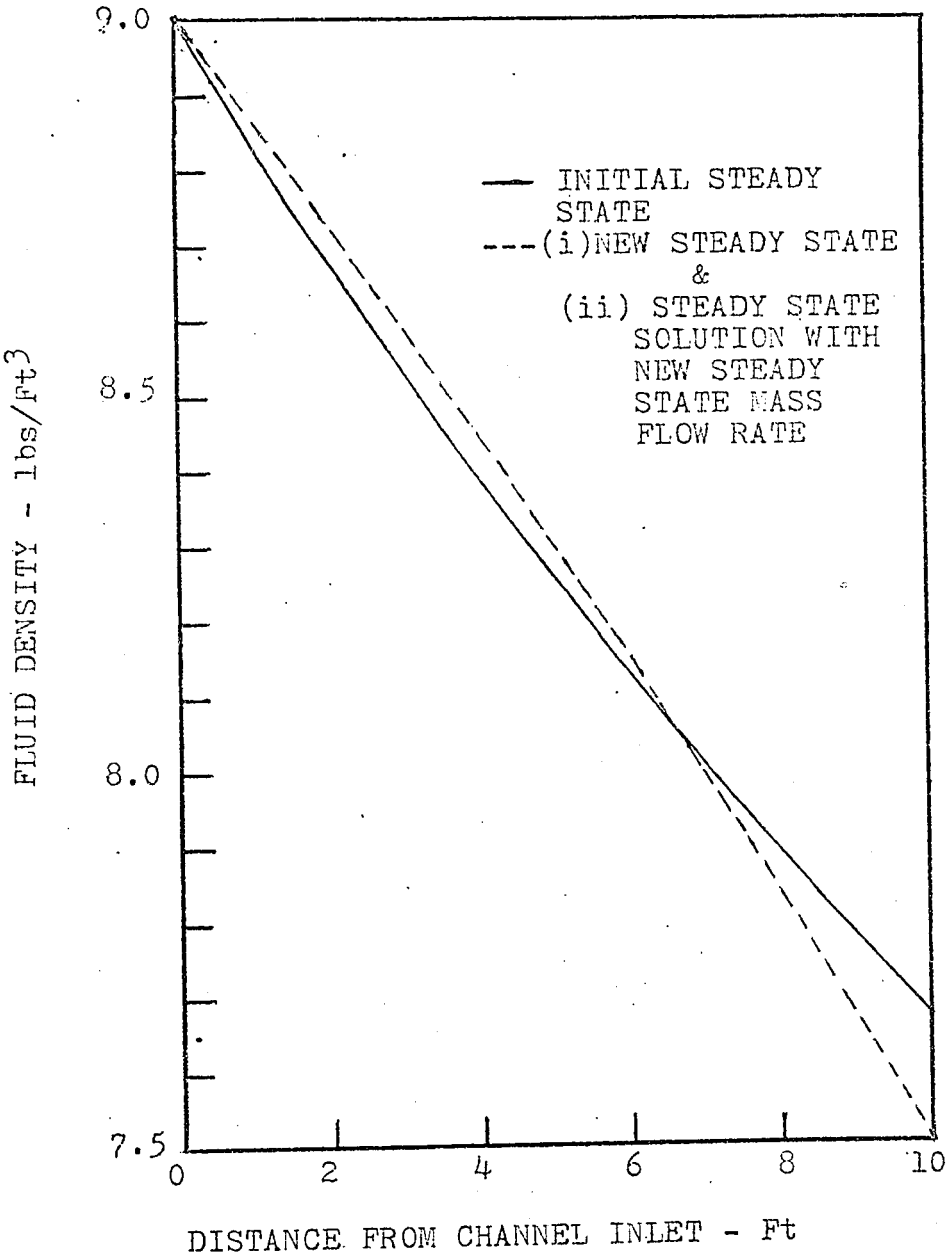

FIG.26: FLUID DENSITY VS. DISTANCE FROM CHANNEL INLET (RUN NO. 6)

APPENDIX A

DERIVATIONS OF EQUATIONS (2.1) and (2.2)

CONTINUITY EQUATION

The law of conservation of mass for the control volume shown in Fig.1(a) can be written as (10)

$$\frac{\partial}{\partial z}(\rho u A)dz = -\frac{\partial}{\partial t}(\rho A dz)$$

or, after simplification, as

$$\frac{\partial \rho}{\partial t} + \rho\frac{\partial u}{\partial z} + u\frac{\partial \rho}{\partial z} = 0 \qquad (A.1)$$

where u represents the flow velocity.

Using G, the mass flow rate, for (ρu) Eq. (A.1) can be written as

$$\frac{\partial \rho}{\partial t} + \frac{\partial G}{\partial z} = 0 \qquad (A.2)$$

MOMENTUM EQUATION

The momentum equation expresses Newton's second law of motion and can be written for the control volume of Fig.1(b) by equating the summation of forces acting on the control volume element in z-direction to the element mass times its acceleration. Thus we obtain (10)

$$PA - \left[PA + \frac{\partial (PA)}{\partial z}dz\right] - \frac{g}{g_c}\rho A dz - \tau_w \pi D dz = \left(\frac{\rho A dz}{g_c}\right)\frac{Du}{Dt} \qquad (A.3)$$

where

$\frac{Du}{Dt} \equiv \frac{\partial u}{\partial t} + u\frac{\partial u}{\partial z}$ represents the acceleration of a particle.

Expanding Eq. (A.3) and dividing throughout by Adz, we obtain

$$-\frac{\partial P}{\partial z} - \frac{g\rho}{g_c} - \frac{\tau_w \pi D}{A} = \frac{\rho}{g_c}\left(\frac{\partial u}{\partial t} + u\frac{\partial u}{\partial z}\right).$$

After simplification, this equation can be written as

$$\rho\frac{\partial u}{\partial t} + \rho u\frac{\partial u}{\partial z} + g_c\frac{\partial P}{\partial z} + g\rho + g_c\tau_w\frac{\pi D}{A} = 0 \qquad (A.4)$$

It is customary to express the wall friction effects by means of a friction factor f with the following equation (7):

$$\frac{\tau_w \pi D}{A} = \frac{(f/\rho)|G|G}{2Dg_c}$$

or

$$\tau_w\frac{\pi D}{A} = \frac{K|G|G}{\rho g_c} \qquad (A.5)$$

where $K = \frac{f}{2D}$ represents the wall friction factor $(ft)^{-1}$.

The product $|G|G$, in this equation, is utilized to obtain a change in the sign of τ_w upon a reversal of flow through the channel.

Substitution of Eq. (A.5) into Eq. (A.4) yields

$$\rho\frac{\partial u}{\partial t} + \rho u\frac{\partial u}{\partial z} + g_c\frac{\partial P}{\partial z} + g\rho + \frac{K|G|G}{\rho} = 0 \qquad (A.6)$$

Replacing ρu by G and their derivatives, Eq. (A.6) takes the following form:

$$\frac{\partial G}{\partial t} - \frac{G}{\rho}\frac{\partial \rho}{\partial t} + \frac{G}{\rho}\frac{\partial G}{\partial z} - \frac{G^2}{\rho^2}\frac{\partial \rho}{\partial z} + g_c\frac{\partial P}{\partial z} + g\rho + \frac{K|G|G}{\rho} = 0$$

Eliminating $\frac{\partial \rho}{\partial t}$ by the use of continuity equation (A.2), we obtain

$$\frac{\partial G}{\partial t} + \frac{2G}{\rho}\frac{\partial G}{\partial z} - \frac{G^2}{\rho^2}\frac{\partial \rho}{\partial z} + g_c\frac{\partial P}{\partial z} + g\rho + \frac{K|G|G}{\rho} = 0$$

which can be rewritten as

$$\frac{\partial G}{\partial t} + \frac{\partial (G^2/\rho)}{\partial z} + g_c\frac{\partial P}{\partial z} + g\rho + \frac{K|G|G}{\rho} = 0 \qquad (A.7)$$

APPENDIX B

COMPUTER PROGRAM

```
C               ***************************
C                       RUN  NO.  1
C               ***************************
C
      IMPLICIT REAL*8(A-H,O-Z)
      DIMENSION G(2,51),ROW(2,51),S(2,51),P(2,51)
2     FORMAT(1H1)
33    FORMAT(1X,D21.14,5X,D21.14,5X,D21.14)
4     FORMAT(1X,I5,5X,D21.14,5X,D21.14,5X,D21.14)
7     FORMAT(1X,'MATRIX=P1BYQ1',///)
47    FORMAT('0',I5,5X,D21.14,5X,D21.14,5X,D21.14,5X,D21.14)
63    FORMAT(//,2X,'S.NO.',15X,'G',25X,'ROW',25X,'S',25X,'P',//)
66    FORMAT(70X,'YYY=',I5)
      INTEGER Q1,P1,CTR,Y,YYY,Z
      REAL  JH
      P1=2000
      Q1=51
      CLENG=10.
      TIME=0.2
      DZ=CLENG/(Q1-1)
      DT=TIME/P1
      AK1=0.06
      GR=32.2
      GAMA=1.4
      JH=778.
      CVO=0.17143
      G0=100.
      P0=2000.*144.
      ROWO=9.0
      S0=0.289308/CVO
      CK=P0/(DEXP(S0)*ROWO**GAMA)
      C=0.0
C     ***************************************************
C
C     INITIAL STEADY STATE SOLUTION
C
C     ***************************************************
C
10    I=1
      DO 11 J=1,Q1
11    G(I,J)=100.0
```

```
      ROW(1,1)=ROW0
      S(1,1)=S0
      P(1,1)=P0/144.
      WRITE(3,2)
      WRITE(3,7)
      WRITE(3,33)ROW(1,1),S(1,1),P(1,1)
      DO 15 J=2,01
      ROW1=ROW0
      S1=S0
      CTR=0
12    X1=(-GR*ROW1)-(AK1*G0*G0/ROW1)
      B=DEXP(S1)
      A=DSQRT(GR*GAMA*(ROW1**(GAMA-1.0))*B*CK)
      QT=(Q+(AK1*G0*G0*G0)/(ROW1*ROW1*ROW1*GR*JH))*(GR*GAMA*
     1(GAMA-1.0)*JH)/(A*A)
      X2=-GR*CK*B*(ROW1**(GAMA+1.))*QT/G0
      X2=(A*A)-(G0*G0/(ROW1*ROW1))
      X2=1/X2
      DROW=(X1+X2)*X2*D7
      DS=QT*ROW1*D7/G0
      IF(CTR.GT.0) GO TO 13
      ROWA=ROW0+DROW
      SA=S0+DS
      ROW1=(ROWA+ROW0)/2
      S1=(SA+S0)/2
      CTR=1
      GO TO 12
13    ROW2=ROW0+DROW
      S2=S0+DS
      IF(DABS(ROWA-ROW2)/ROWA.GT..0001) GO TO 23
      IF(DABS(SA-S2)/SA.LT..000001) GO TO 14
23    ROW1=(ROW1+ROW2)/2
      S1=(S0+S2)/2
      ROWA=ROW2
      SA=S2
      GO TO 12
14    ROW(1,J)=ROW2
      S(1,J)=S2
      P(1,J)=DEXP(S(1,J))*CK*ROW(1,J)**GAMA/144.0
      WRITE(3,4)J,ROW(1,J),S(1,J),P(1,J)
      ROW1=ROW2
      S1=S2
      ROW0=ROW2
      S0=S2
```

```
      CTR=0
15    CONTINUE
C
C*****************************************************************
C
C     TRANSIENT SOLUTION (INLET STATION)
C
C*****************************************************************
C
      GDROP=100.0*DT/70.2
      YYY=0
      Z=0
      Y=0
      I=2
99    DO 40 J =1,Q1
      IF(J.GT.1) GO TO 17
      CTR=0
      G3=G(I-1,J)-GDROP
      ROW3=ROW(I-1,J)
      S3=S(I-1,J)
      AL=DT*G(I-1,J)
      BE=DT*(G(I-1,J+1)-G(I-1,J))/DZ
      GAM=ROW(I-1,J)
      ETA=(ROW(I-1,J+1)-ROW(I-1,J))/DZ
      E=DEXP(S3)
      A=DSQRT(G3*GAMA*(ROW3**(GAMA-1.0))*E*CK)
22    C1=DT*((G3/ROW3)-2*A)
      B=(2*GAM+BE+C1*ETA)/(2*ETA)
      C=(AL+C1*GAM)/(2*ETA)
      H=-B+DSQRT(B*B-4*C)
      H=H/2
      H1=-B-DSQRT(B*B-4*C)
      H1=H1/2
      IF(H1.LT.0.0) GO TO 9
      H=H1
9     DG=G3-(G(I-1,J)+H*(G(I-1,J+1)-G(I-1,J))/DZ)
      X1=G(I-1,J)+H*(G(I-1,J+1)-G(I-1,J))/DZ
      X2=ROW(I-1,J)+H*(ROW(I-1,J+1)-ROW(I-1,J))/DZ
      GP=(X1/X2+G3/ROW3)/2
      ROWN=ROW3+ROW(I-1,J)+H*(ROW(I-1,J+1)-ROW(I-1,J))/DZ
      ROWN=ROWN/2
      SN=S3+S(I-1,J)+H*(S(I-1,J+1)-S(I-1,J))/DZ
      SN=SN/2
      P=DEXP(SN)
```

```
      A=DSQRT(GR*GAMA*(ROWN**(GAMA-1.0))*E**CK)
      GP=GP+A
      DS=S3-(S(I-1,J)+H*(S(I-1,J+1)-S(I-1,J))/DZ)
      GAV=G3+G(I-1,J)+H*(G(I-1,J+1)-G(I-1,J))/DZ
      GAV=GAV/2
      AGAV=DABS(GAV)
      DT=(C+(AK1*GAV*GAV*AGAV)/(ROWN*ROWN*ROWN*GR*JH))*(GR*GAMA*
     1(GAMA-1.0)*JH)/(A*A)
      PRP=A*ROWN/GAMA
      FP=GR*ROWN+AK1*GAV*AGAV/ROWN
      FP=FP+PRP*DT
      DROW=DG-PRP*DS+FP*DT
      DROW=DROW/GP
      ROW3=ROW(I-1,J)+H*(ROW(I-1,J+1)-ROW(I-1,J))/DZ+DROW
      IF(CTR.GT.0) GO TO 111
      ROW0=ROW3
      CTR=1
      GO TO 22
111   IF(DABS(ROW3-ROW0)/ROW0.LT..0001) GO TO 25
      ROW0=ROW3
      GO TO 22
25    G(I,J)=G3
      ROW(I,J)=ROW3
      S(I,J)=S3
      P(I,J)=DEXP(S(I,J))*CK*ROW(I,J)**GAMA/144.0
      GO TO 40
C
C     ***********************************************************
C
C     TRANSIENT SOLUTION (INTERIOR STATIONS)
C
C     ***********************************************************
C
17    IF(J.EQ.01) GO TO 45
      CTR=0
      G(I,J)=G(I-1,J)
      ROW(I,J)=ROW(I-1,J)
      S(I,J)=S(I-1,J)
      V11=(G(I-1,J+1)-G(I-1,J))/DZ
      V22=(ROW(I-1,J+1)-ROW(I-1,J))/DZ
      AL1=-(G(I-1,J)*DT)
      BE1=-(V11*DT)
      GA2=2*ROW(I-1,J)
      BTA1=2*V22
```

```
      V1=(G(I-1,J-1)-G(I-1,J))/DZ
      V2=(ROW(I-1,J-1)-ROW(I-1,J))/DZ
      AL=G(I-1,J)*DT
      BE=V1*DT
      ETA=2*V2
      E=DEXP(S(I,J))
      AP=DSQRT(GR*GAMA*(ROW(I,J)**(GAMA-1.0))*E**CK)
      AM=AP
24    C1=DT*(AM-G(I,J)/(2*ROW(I,J)))
      B=(GA-BE-C1*ETA1)/ETA1
      C=(-AL-C1*GA)/ETA1
      H=-B+DSQRT(B*B-4*C)
      H=H/2
      H1=-B-DSQRT(B*B-4*C)
      H1=H1/2
      IF(H1.LT.0.0) GO TO 26
      H=H1
26    C1=DT*(AP+G(I,J)/(2*ROW(I,J)))
      B=(GA-BE-C1*ETA)/ETA
      C=(-AL-C1*GA)/ETA
      AK=-B+DSQRT(B*B-4*C)
      AK=AK/2
      AK11=-B-DSQRT(B*B-4*C)
      AK11=AK11/2
      IF(AK11.LT.0.0) GO TO 28
      AK=AK11
28    C1=DT*G(I,J)/(2*ROW(I,J))
      B=(GA-BE-C1*ETA)/ETA
      C=(-AL-C1*GA)/ETA
      W=-B+DSQRT(B*B-4*C)
      W=W/2
      W1=-B-DSQRT(B*B-4*C)
      W1=W1/2
      IF(W1.LT.0.0) GO TO 29
      W=W1
29    G3=G(I,J)
      ROW3=ROW(I,J)
      S3=S(I,J)
      G2=G(I-1,J)+AK*(G(I-1,J-1)-G(I-1,J))/DZ
      ROW2=ROW(I-1,J)+AK*(ROW(I-1,J-1)-ROW(I-1,J))/DZ
      S2=S(I-1,J)+AK*(S(I-1,J-1)-S(I-1,J))/DZ
      G1=G(I-1,J)+H*(G(I-1,J+1)-G(I-1,J))/DZ
      ROW1=ROW(I-1,J)+H*(ROW(I-1,J+1)-ROW(I-1,J))/DZ
      S1=S(I-1,J)+H*(S(I-1,J+1)-S(I-1,J))/DZ
```

```
      GP2=G(I-1,J)+W*(G(I-1,J-1)-G(I-1,J))/DZ
      ROWP2=ROW(I-1,J)+W*(ROW(I-1,J-1)-ROW(I-1,J))/DZ
      SP2=S(I-1,J)+W*(S(I-1,J-1)-S(I-1,J))/DZ
      GP=(G2+G3)/2
      AGP=DABS(GP)
      GM=(G1+G3)/2
      AGM=DABS(GM)
      GP22=(GP2+G3)/2
      AGP22=DABS(GP22)
      RP=(ROW2+ROW3)/2
      RM=(ROW1+ROW3)/2
      RP2=(ROWP2+ROW3)/2
      GRP=(G3/ROW3+G2/ROW2)/2.
      GRM=(G3/ROW3+G1/ROW1)/2
      SP=(S2+S3)/2
      SM=(S1+S3)/2
      SP2P=(SP2+S3)/2
      E=DEXP(SP)
      AP=DSQRT(GR*GAMA*(PP**(GAMA-1.0))*E*CK)
      E=DEXP(SM)
      AM=DSQRT(GR*GAMA*(RM**(GAMA-1.0))*E*CK)
      E=DEXP(SP2P)
      AP2=DSQRT(GR*GAMA*(RP2**(GAMA-1.0))*E*CK)
      QT=(Q+(AK1*GP22*GP22*AGP22)/(RP2*RP2*RP2*GR*JH))*
     1(GR*GAMA*(GAMA-1.0)*JH)/(AP2*AP2)
      S3=SP2+QT*DT
      ERP=(RP*AP)/GAMA
      QT=(Q+(AK1*GP*GP*AGP)/(RP*RP*PP*GR*JH))*
     1(GR*GAMA*(GAMA-1.0)*JH)/(AP*AP)
      EP=GP*RP+AK1*GP*AGP/RP
      EP=EP-RRP*QT
      ERM=(RM*AM)/GAMA
      QT=(Q+(AK1*GM*GM*AGM)/(RM*RM*RM*GR*JH))*
     1(GR*GAMA*(GAMA-1.0)*JH)/(AM*AM)
      EM=GR*RM+AK1*GM*AGM/RM
      EM=EM+RRM*QT
      X1=(GRP-AP)*ROW2-G2+EP*DT-RRP*S2
      X2=-(GRM+AM)*ROW1+G1-EM*DT-RRM*S1
      DEN=(AP+AM)-(GRP-GRM)
      DEN=-DEN
      ROW3=(X1+X2+(RRP+RRM)*S3)/DEN
      G3=-X1+(GRP-AP)*ROW3-RRP*S3
      IF(CTR.GT.0) GO TO 20
      CTR=1
```

```
19      S(I,J)=S3
        ROW(I,J)=ROW3
        G(I,J)=G3
        GO TO 24
20      IF(DABS((G3-G(I,J))/G(I,J)).GT..0001) GO TO 19
        IF(DABS((ROW3-ROW(I,J))/ROW(I,J)).LT..0001.AND.
     1  DABS((S3-S(I,J))/S(I,J)).LT..0001) GO TO 21
        GO TO 19
21      S(I,J)=S3
        G(I,J)=G3
        ROW(I,J)=ROW3
        P(I,J)=DEXP(S(I,J))*CK*ROW(I,J)**GAMA/144.0
        GO TO 40
C
CCC     ***********************************************************
CCC
CCC     TRANSIENT SOLUTION (DISCHARGE STATION)
CCC
CCC     ***********************************************************
C
45      CTR=0
        G3=G(I-1,J)
        ROW3=ROW(I-1,J)
        S3=S(I-1,J)
        GO=G(I-1,J)
        ROWO=ROW(I-1,J)
        SO=S(I-1,J)
        G1=G(I-1,J-1)
        ROW1=ROW(I-1,J-1)
        S1=S(I-1,J-1)
        GD=G1-GO
        ROWD=ROW1-ROWO
        SD=S1-SO
        AL=GO*DT
        BE=GD*DT/DZ
        GA1=ROWO
        ETA=ROWD/DZ
        E=DEXP(S3)
        AP=DSQRT(GR*GAMA*(ROW3**(GAMA-1.0))*E*CK)
31      C1=DT*((G3/ROW3)+2*AP)
        B=(2*GA1-BE-C1*ETA)/(2*ETA)
        C=-(AL+C1*GA1)/(2*ETA)
        AK=-B+DSQRT(B*B-4*C)
        AK=AK/2
```

```
      AK11=-B-DSQRT(B*B-4*C)
      AK11=AK11/2
      IF(AK11.LT.0.0) GO TO 30
      AK=AK11
   30 C1=DT*G3/ROW3
      B=(2*GA1-BE-C1*ETA)/(2*ETA)
      C=-(AL+C1*GA1)/(2*ETA)
      W=-B+DSQRT(B*B-4*C)
      W=W/2
      W1=-B-DSQRT(B*B-4*C)
      W1=W1/2
      IF(W1.LT.0.0) GO TO 36
      W=W1
   36 G2=G0+AK*GD/DZ
      ROW2=ROW0+AK*ROWD/DZ
      S2=S0+AK*SD/DZ
      GP2=G0+W*GD/DZ
      ROWP2=ROW0+W*ROWD/DZ
      SP2=S0+W*SD/DZ
      GP=(G2+G3)/2
      AGP=DABS(GP)
      GP22=(GP2+G3)/2
      AGP22=DABS(GP22)
      RP=(ROW2+ROW3)/2
      RP2=(ROWP2+ROW3)/2
      GRP=(G3/ROW3+G2/ROW2)/2
      SP=(S2+S3)/2
      SP2P=(SP2+S3)/2
      E=DEXP(SP)
      AP=DSQRT(GR*GAMA*(RP**(GAMA-1))*E*CK)
      E=DEXP(SP2P)
      AP2=DSQRT(GR*GAMA*(RP2**(GAMA-1.0))*E*CK)
      QT=(C+(AK1*GP22*GP22*AGP22)/(RP2*RP2*RP2*(GR*JH))*
     1(GR*GAMA*(GAMA-1.0)*JH)/(AP2*AP2)
      S3=SP2+QT*DT
      RRP=(RP*AP)/GAMA
      QT=(C+(AK1*GP*GP*AGP)/(RP*RP*RP*GR*JH))*
     1(GR*GAMA*(GAMA-1.0)*JH)/(AP*AP)
      FP=GR*PP+AK1*GP*AGP/RP
      FP=FP-RRP*QT
      X1=(GRP-AP)*ROW2-G2+FP*DT-RRP*S2
      G3=-X1+(GRP-AP)*ROW3-RRP*S3
      IF(CTR.GT.0) GO TO 22
      G00=G3
```

```
      S00=S3
      CTR=1
      GO TO 31
32    IF(DABS((G3-G00)/G3).GT..0001)GO TO 31
      IF(DABS((S3-S00)/S3).LT..0001) GO TO 35
      G00=G3
      S00=S3
      GO TO 31
35    S(I,J)=S3
      G(I,J)=G3
      ROW(I,J)=ROW3
      P(I,J)=DEXP(S(I,J))*CK*ROW(I,J)**GAMA/144.
40    CONTINUE
      Z=Z+1
      IF(Z.NE.20) GO TO 50
      YYY=YYY+1
      WRITE(3,66)YYY
      WRITE(3,63)
      DO 44 J=1,01
      WRITE(3,47)J,G(I,J),ROW(I,J),S(I,J),P(I,J)
44    CONTINUE
      Z=0
50    DO 55 J=1,01
      G(I-1,J)=G(I,J)
      ROW(I-1,J)=ROW(I,J)
      S(I-1,J)=S(I,J)
55    CONTINUE
      Y=Y+1
      IF(Y.LT.2001) GO TO 99
      RETURN
      END
```

REFERENCES

1. Courant, R. and Friedrichs, K. O., "Supersonic Flow and Shock Waves," Interscience Publishers, Inc., New York, 1948, Vol. 1.

2. Gorman, D. J. and D'Arcy, D. F., "A Fixed-Grid Method of Characteristics for Predicting One-Dimensional Flow Transients," Report No. CRNL-592, Atomic Energy of Canada Ltd., February 1971, (Unpublished).

3. Haller, P. de, "Graphical Method for the Analysis of Gas Dynamic Problems," Engineers Digest, Vol. 6, No. 9, September 1945, pp.225-230.

4. Jenny, E., "Unidimensional Transient Flow with Consideration of Friction, Heat Transfer, and Change of Section," Brown Boveri Review, Vol. 37, No. 11, 1950, pp.447-461.

5. Kahane, A. and Lees, L., "Unsteady One-Dimensional Flows with Heat Addition or Entropy Gradients," Journal of the Aeronautical Sciences, Vol. 15, No. 11, Nov. 1948, pp.665-670.

6. Keenan, J. H. and Kaye, J., "Gas Tables", John Wiley and Sons, Inc., New York, 1948.

7. Meyer, J. E., "Conservation Laws in One-Dimensional Hydrodynamics," Bettis Technical Review, WAPD-BT-20, September 1960, pp.61-72.

8. Moody, L. F., "Friction Factors for Pipe Flow," Transactions, A.S.M.E., Vol. 66, Nov. 1944, pp.671-684.

9. Rudinger, G., "Wave Diagrams for Nonsteady Flow in Ducts," D. Van Nostrand Company, Inc., 1955.

10. Stoner, M. A., "Analysis and Control of Unsteady Flows in Natural Gas Piping Systems," Transactions of the ASME, Journal of Basic Engineering, Sept. 1969, pp.331-340.